

Improved Design of a Cartridge-Type Helical Blanket System for the Helical Fusion Reactor FFHR-b1

Junichi MIYAZAWA^{1,2)}, Hitoshi TAMURA¹⁾, Teruya TANAKA^{1,2)}, Yukinori HAMAJI¹⁾, Makoto KOBAYASHI¹⁾, Takanori MURASE¹⁾, Sho NAKAGAWA¹⁾, Takuya GOTO^{1,2)}, Nagato YANAGI^{1,2)}, Akio SAGARA^{1,2)} and the FFHR Design Group

¹⁾National Institute for Fusion Science, 322-6 Oroshi, Toki, Gifu 509-5292, Japan

²⁾SOKENDAI (The Graduate University for Advanced Studies), 322-6 Oroshi, Toki, Gifu 509-5292, Japan

(Received 26 July 2019 / Accepted 24 October 2019)

The cartridge-type helical blanket system called the CARDISTRY-B has been proposed for the helical fusion reactor FFHR-d1. The CARDISTRY-B is aimed at easy construction and maintenance. However, there remain many issues in the design. For example, these include a large number of cartridges, no tangential ports, low compatibility with the helical divertor, and others. To solve these issues, an improved design of the cartridge-type blanket is proposed and named the CARDISTRY-B2. This is composed of the tritium breeding blanket (BB) filled with the flowing molten salt and the neutron shielding blanket (SB) filled with the tungsten-carbide. The number of the BB (or, SB) cartridges in the 1/10 section of the full torus are reduced from 32 to 17 (or, from 44 to 17). Tangential ports for the neutral beam injection heating are newly equipped together with the multi-purpose blanket cartridge. Compatibility with the helical divertor is also improved. The BB cartridges are fixed on the fixing units set on the top of the SB. No other part of the BB is touching the SB except the fixing ribs. The SB cartridges surround the superconducting magnet coils and work as the cryostat inside the vacuum vessel. This makes the large bellows for the large maintenance ports unnecessary. Details of the CARDISTRY-B2 designed for a small helical fusion reactor FFHR-b1 are described in this paper.

© 2019 The Japan Society of Plasma Science and Nuclear Fusion Research

Keywords: heliotron, fusion reactor, molten salt blanket, neutron shield, thermal shield, LHD, FFHR

DOI: 10.1585/pfr.14.1405163

1. Introduction

The FFHR-d1 is the LHD-type helical fusion reactor aiming at demonstration of the fusion output, P_{fusion} , of ~ 3 GW and the device lifetime of longer than 30 years [1]. The device size is four times larger than the LHD [2], *i.e.*, the major radius of the helical coils, R_c , is 15.6 m in the FFHR-d1 and 3.9 m in the LHD. The magnetic field strength at the helical coil center, B_c , is 4.7 T–5.6 T. The FFHR-c1 is the compact version of the FFHR-d1 with 0.7 times smaller device size ($R_c = 10.92$ m) [3]. The FFHR-c1 is aiming at demonstration of one-year steady-state operation with self-produced fuel and electricity. The B_c is increased to 7.3 T to achieve a good plasma confinement in the small device. There are 22 important issues to be solved to realize the FFHR-c1 and d1 [4]. To effectively resolve these issues, a step-by-step strategy has been proposed [4]. In this strategy, the FFHR-b1 as the helical volumetric neutron source (HEVNS) and the FFHR-a1 as the pilot-HEVNS are planned before the FFHR-c1. The FFHR-b1 has the same device size as the LHD ($R_c = 3.9$ m), with $B_c = 5.7$ T. The main purpose of the FFHR-b1 is to demonstrate new technologies of, for example, high-temperature superconducting (HTS) mag-

net coils, and a cartridge-type blanket system, which is the main topic of this paper, in a reactor-relevant condition. Tangential neutral beam injection (NBI) is the main plasma heating method in the FFHR-b1. The neutrons produced by the beam-plasma fusion irradiate the SC magnet coils and the blankets. From this point of view, the FFHR-b1 plays the role of the component test facility. The FFHR-b1 can also be a commercial neutron source. The FFHR-a1 is the non-nuclear R&D device of 0.7 times smaller device size ($R_c = 2.73$ m) than the FFHR-b1, with $B_c = 4.0$ T.

The blanket is one of the important components comprising the fusion reactor. The blanket has three roles of tritium breeding, neutron shielding, and energy conversion from the 14 MeV neutron energy to the thermal energy. Because of the severe neutron irradiation [5], the blanket should be maintained periodically. At the same time, RAMI (reliability, availability, maintainability, and inspectability) should be satisfied in the blanket at a high level. In the case of the helical reactor, how to construct the complicated structure within a realistic period of time is also an important issue. To realize easy construction and maintenance, a cartridge-type helical blanket system named the CARDISTRY-B (cartridges divided and inserted radially - blanket) has been proposed [3, 6] based

author's e-mail: miyazawa.junichi@nifs.ac.jp

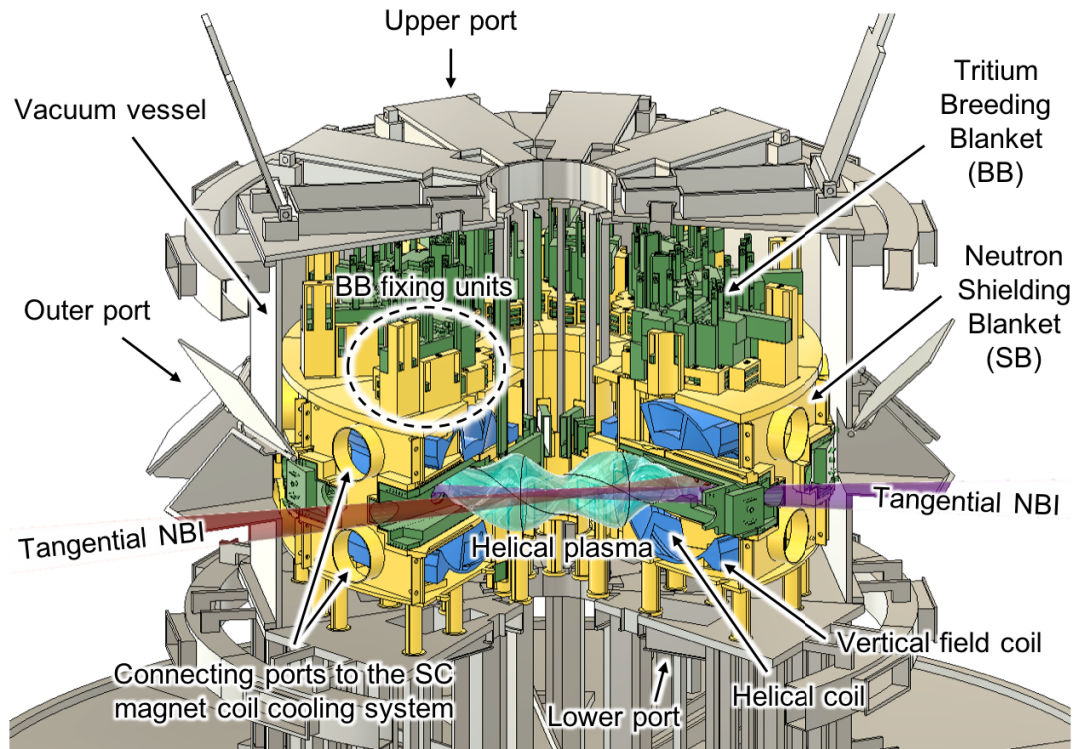


Fig. 1 Schematic view of the CARDISTRY-B2 for the FFHR-b1.

on the T-SHELL blanket concept [7]. The CARDISTRY-B is composed of the tritium breeding blanket (BB) filled with the flowing molten salt and the neutron shielding blanket (SB) filled with the tungsten carbide (WC). Both of the BB and SB are toroidally segmented every two degrees. At each toroidal angle, the segmented parts are divided into several cartridges in order to make it possible to assemble the cartridges after construction of the SC magnet coils. A detailed maintenance process of the CARDISTRY-B has been discussed and the availability is estimated to be $\sim 70\%$ [3]. The thermal and flow analysis in a typical cartridge has been performed [8]. The neutron transport simulation also has begun [9].

Although the CARDISTRY-B has enabled detailed discussions on the maintenance scenario and numerical simulations, there remain many unsatisfactory points, as listed below:

- (1) a large number of cartridges (32 BB cartridges and 44 SB cartridges in a 1/10 section of the full torus),
- (2) no tangential ports available for tangential NBI,
- (3) low compatibility with the helical divertor,
- (4) extremely large bellows are indispensable for large maintenance ports,

and others. To solve these unsatisfactory points, an improved design of the cartridge-type blanket is proposed and named the CARDISTRY-B2. In this paper, details of the CARDISTRY-B2 applied for the FFHR-b1 as the HEVNS are described. An overview of the CARDISTRY-

B2 is given in the next Section. Detailed explanations on the BB and SB cartridges are given in Secs. 3 and 4, respectively. Compatibility with the divertor is discussed in Sec. 5. Summary and issues remaining for future studies are given in Sec. 6.

2. Overview of the CARDISTRY-B2

A schematic view of the CARDISTRY-B2 applied to the FFHR-b1 is shown in Fig. 1. Tangential ports for the tangential NBI are newly equipped. These are inevitable especially in the case of FFHR-b1 as the HEVNS to produce the beam-plasma fusion neutrons. The CARDISTRY-B2 is composed of 17 BB and 17 SB cartridges as shown in Figs. 2 and 3, respectively, in a 1/10 section of the full torus of the FFHR-b1. In total, 170 BB and 170 SB cartridges are used in the CARDISTRY-B2. Compared with the former CARDISTRY-B, the total number of the cartridges are largely reduced from 760 to 340. Among these, 14 BB cartridges of B01 - BB13, and BB17, *i.e.*, 140 BB cartridges in total, need periodical maintenance. These BB cartridges are equipped with the divertor units, as will be explained later in Sec. 5. Therefore, the divertor units are replaced together with the 140 BB cartridges. This number is equivalent to the total number of the components that need periodical maintenance in the tokamak DEMO of 128, which consists of 80 blanket segments and 48 divertor cassettes [10, 11]. The other BB cartridges of BB14 - BB16 can be replaced if necessary. The SB cartridges are basically used during the whole device life. Nine BB cartridges

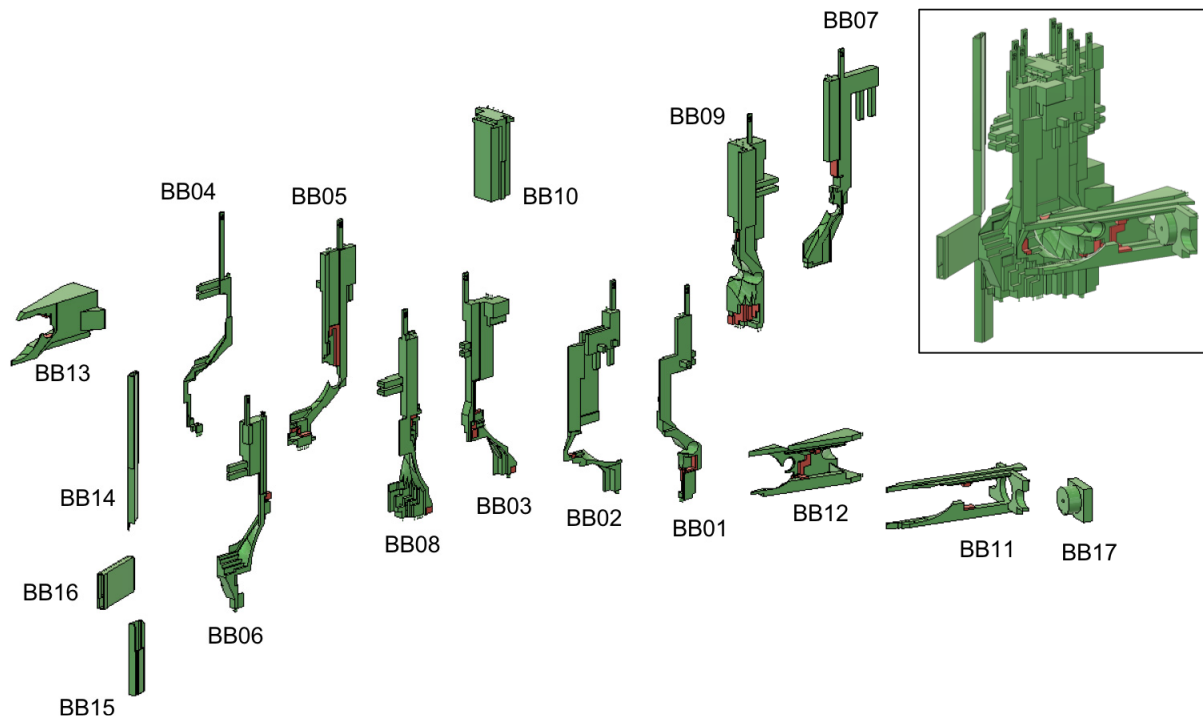


Fig. 2 Exploded view of the BB cartridges in a 1/10 section. Assembled view is shown in the box at the upper right-top.

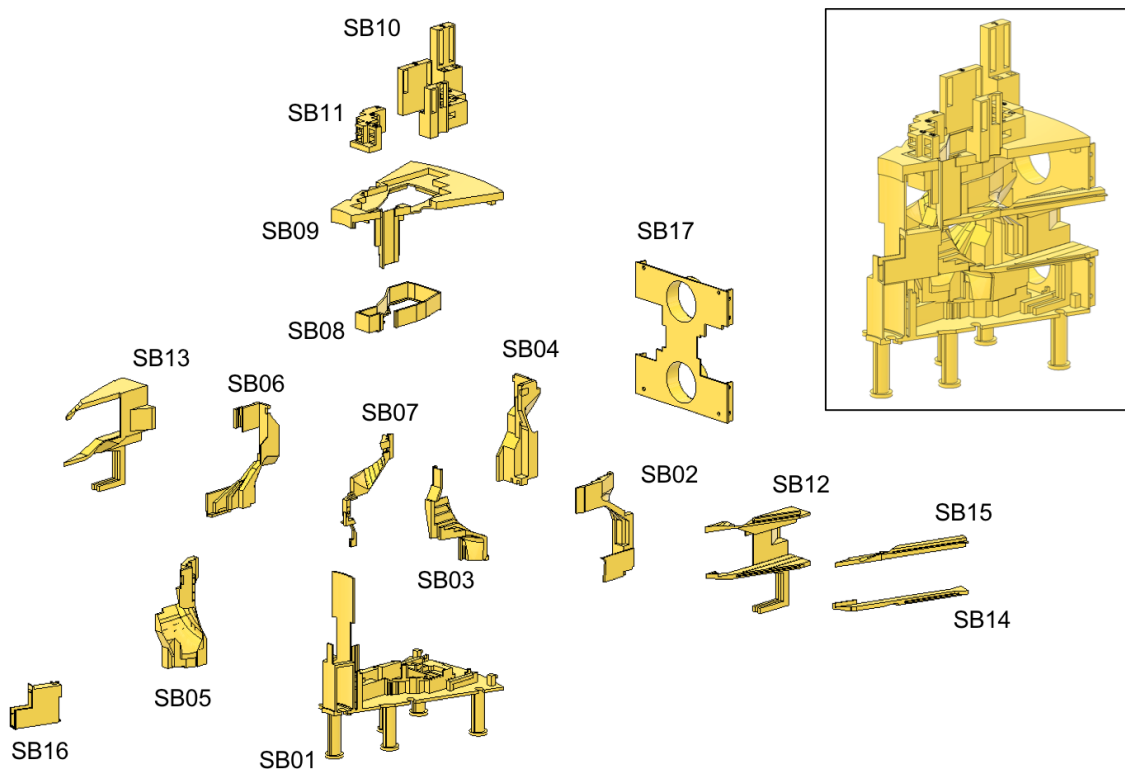


Fig. 3 Exploded view of the SB cartridges in a 1/10 section. Assembled view is shown in the box on the upper right-top.

of BB01 - BB09 are fixed to the fixing units of SB10 and SB11 equipped on the top of the SB cartridges (see Fig. 1). No other part of these BB cartridges touches the SB except the fixing ribs (see Fig. 6 in the next section, and see also

Figs. B1 - B9 in the Appendix).

The SB cartridges completely enclose the SC magnet coils. Surfaces of the SB cartridges facing the SC magnet coils are cooled down to ~ 80 K by gas He and these

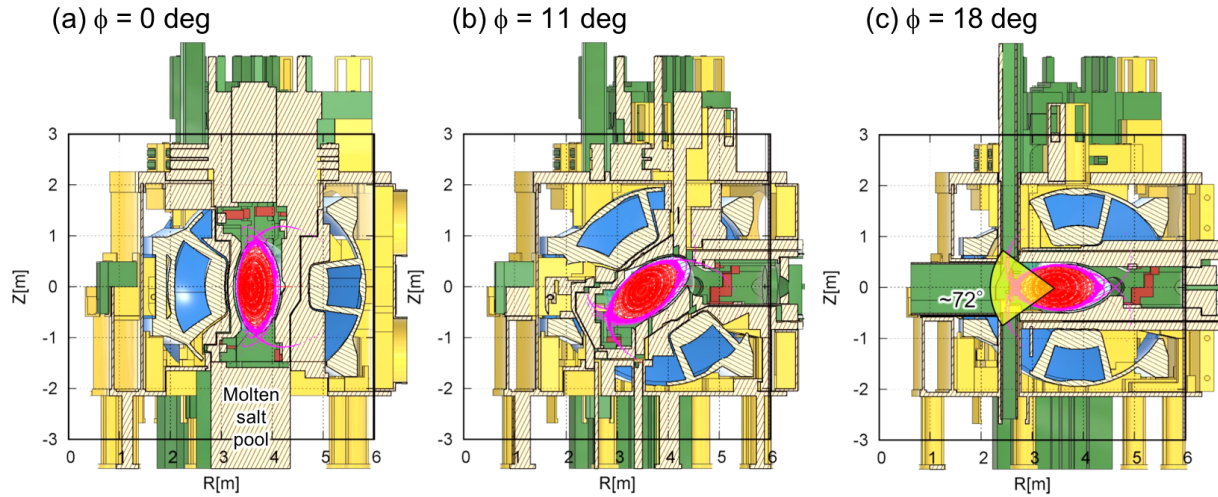


Fig. 4 Sliced views of the CARDISTRY-B2 with the Poincaré plot of the magnetic field lines at the toroidal angle $\phi = 0, 11$, and 18 deg.

works as the thermal shield for the SC magnets. In the LHD, similar thermal shield is set on the inner surface of the cryostat and the main vacuum vessel for plasma confinement is placed inside the cryostat. In this case, large-size bellows are needed to connect the ports on the cryostat to the main vacuum vessel. In the case of the fusion reactor as the FFHR-b1, c1, and d1, large maintenance ports, which are relatively larger than the corresponding ports in the LHD, are equipped. Although these large ports are favorable for easy maintenance, there emerges another problem, *i.e.*, such large bellows that can cover the extremely large maintenance ports for the FFHR-d1 will not be available. However, if the cryostat is inside the main vacuum vessel, as in the case of the FFHR-b1 shown in Fig. 1, the large bellows become unnecessary except the connecting ports to the SC magnet coil cooling system, which can be reasonably small.

One of the difficult points in designing a helical fusion reactor is the narrow blanket space at the inboard side of the torus. Sliced views of the CARDISTRY-B2 at the toroidal angle, ϕ , of 0, 11, and 18 degrees are shown in Fig. 4. Other sliced views at different ϕ are shown in Figs. A1 - A4 in the Appendix. As seen in these figures, the blanket space between the plasma including the ergodic layer and the helical coils (HC) is quite narrow at the inboard side of the torus. Nevertheless, the thickness of the BB is kept larger than 100 mm even in the case of the CARDISTRY-B2 for the relatively small FFHR-b1. To maintain this minimum thickness, the BB and SB cartridges are designed using the solids defined at 0 - 20 mm from the HC surface, 0 - 40 mm, 40 - 140 mm (not shown), and 140 - 160 mm from the last-closed-flux-surface (LCFS), as shown in Fig. 5. For example, the plasma side of the BB08 is determined so as to have no interference with the solid defined at 0 - 40 mm from the LCFS, and the thickness of the BB08 is determined by using the solid defined at 40 - 140 mm from the LCFS. Sim-

ilarly, the BB side of the SB05 is determined so as to have no interference with the solid defined at 140 - 160 mm from the LCFS, and the HC side of the SB05 is determined so as to have no interference with the solid defined at 0 - 20 mm from the HC surface. By applying this drawing rule for all other blankets, the clearances between HC-SB, SB-BB, and BB-LCFS are kept 20 mm, 20 mm, and 40 mm, respectively, and the minimum thickness of the BB is kept larger than 100 mm (see Fig. 5 (c)).

At this moment, the clearances between the adjoining cartridges are set to be ≥ 10 mm for both the BB and the SB (see Fig. 5 (c)), to allow a few mm of manufacturing errors and the deformation due to the large temperature change during the operation. These clearances will be reconsidered in the future study, by taking the numerical simulation results on the neutron streaming into account.

3. The Tritium Breeding Blanket (BB)

One of the main roles of the BB is to produce tritium from lithium. In the CARDISTRY-B2, the molten salt including lithium (FLiNaBe, or FLiBe) is used for this. It is also necessary to increase the molten salt temperature high enough for electricity generation. At the same time, the first-wall of the BB facing on the plasma suffers from severe irradiation by charge-exchanged neutrals and neutrons. Therefore, a strong first-wall cooling ability is also required for the BB. In the former study, the thermal and flow analysis on the CARDISTRY-B applied to the FFHR-c1 has been performed [8]. In that study, a flowing channel of 30 mm width is assumed in the plasma facing side of a BB cartridge. Be pebbles are filled inside the BB cartridge as the neutron multiplier. The metal Be pebbles are also beneficial to increase the effective thermal conductivity inside the BB cartridge. The molten salt flows in the SB facing side of the BB at first, and then returns in the 30 mm flowing channel at a higher flow velocity. In this

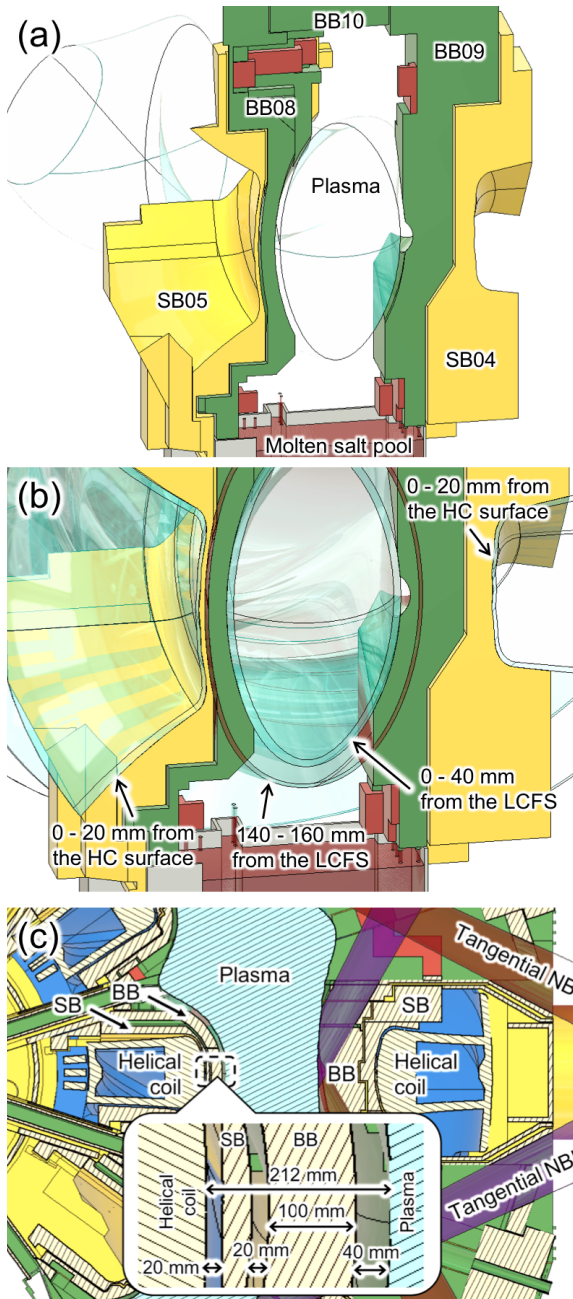


Fig. 5 (a) The plasma and cartridges of SB04, SB05, BB08, BB09, BB10, and the molten salt pool sliced at $\phi = 0$ deg. (b) Solids used to cut the cartridges defined at 0 - 20 mm from the HC surface, 0 - 40 mm and 140 - 160 mm from the LCFS, respectively. (c) Top view of the equatorial slice.

study, we also assume a 30 mm width flowing channel in the plasma facing side (front-side) of each BB cartridge, instead of 2.8 times smaller width, to maintain the similar flow condition with the former study. An exploded view of the BB01 is shown in Fig. 6. See also Figs. B1 - B19 in the Appendix for other BB blankets. The BB cartridges are basically composed of a main case, a separating plate, and a front panel. The molten salt flows in two flow chan-

nels in the front-side and in the back-side of the separating plate. As was discussed above, the thickness of the front-side molten salt is basically fixed to 30 mm, while the back-side molten salt flows through the entire area between the separating plate and the main case. One of the largest differences compared with the former study is that the molten salt flows from the top to the bottom of a BB cartridge in a once-through manner. The molten salt is then released into to the molten salt pool (see Figs. 4 and 5 (a)) from the exhaust pipes equipped on the bottom of each BB cartridge (Fig. 7). Although a quantitative evaluation of the influence of the molten salt vapor, which is lower than 0.1 Pa in the case of FLiBe at 550°C [12], to the plasma remains for future study, we assume that there will be no critical influence since the molten salt consists of the only light weight atoms of F, Li, Na, and Be. When the molten salt containing tritium is released to a vacuum, a part of tritium is also expected to be released into the vacuum because of the low hydrogen solubility of molten salt. This should be also investigated in the future study.

In the CARDISTRY-B2, a multi-purpose blanket (BB17) is prepared in the outer port. The outer port equipped with two tangential ports is composed of three BB blankets, BB11, BB12, and BB13. The BB17 is a plug blanket to be put into a large hole of the BB11, as shown in Fig. 8. It is relatively easy to remove and reinstall the BB17. One can use this as the test blanket module to test other types of blanket using, for example, ceramic pebbles, or liquid metals. It is also possible to use this BB17 for reprocessing of spent nuclear fuel and/or isotope production, for example. By opening a hole on the BB17 as in Fig. 8, it becomes possible to extract neutron beams to distant rooms for medical use, for example.

The coverage is one of the important properties of the blanket. The coverage can be given by the average of the poloidal angle covered by the blanket measured at every toroidal angle. In the case of the CARDISTRY-B2, the poloidal angles that are not covered by the BB cartridges are ~ 80 , ~ 75 , ~ 72 , ~ 70 , and ~ 50 degrees at $\phi = 16, 17, 18, 19$, and 20 degrees, respectively, as shown in Figs. A2 (h), A2 (i), A3 (a), A3 (b), and A3 (c) in the Appendix. At the toroidal angle other than $\phi = 16 - 20$ degrees, the poloidal angle that is not covered by the BB cartridges is zero. Therefore, the coverage is estimated as $1.0 - (80 + 75 + 72 + 70 + 50)/360/36 \sim 0.973$. Note that this estimation does not include the opening area of the tangential ports, the spaces between the adjoining BB cartridges, the thickness of walls and ribs, which are difficult to measure in the toroidal slices as seen in Figs. A1 - A4 in the appendix. Nevertheless, this rough estimation is still acceptable since the tangential ports are located at relatively separated positions, and the number of them will be limited to 4 in the FFHR-b1. Because of the limited space around the FFHR-b1, it is difficult to place many large NBI devices more than 4. Detailed estimation of the tritium breeding ratio (TBR) that is closely related to the coverage

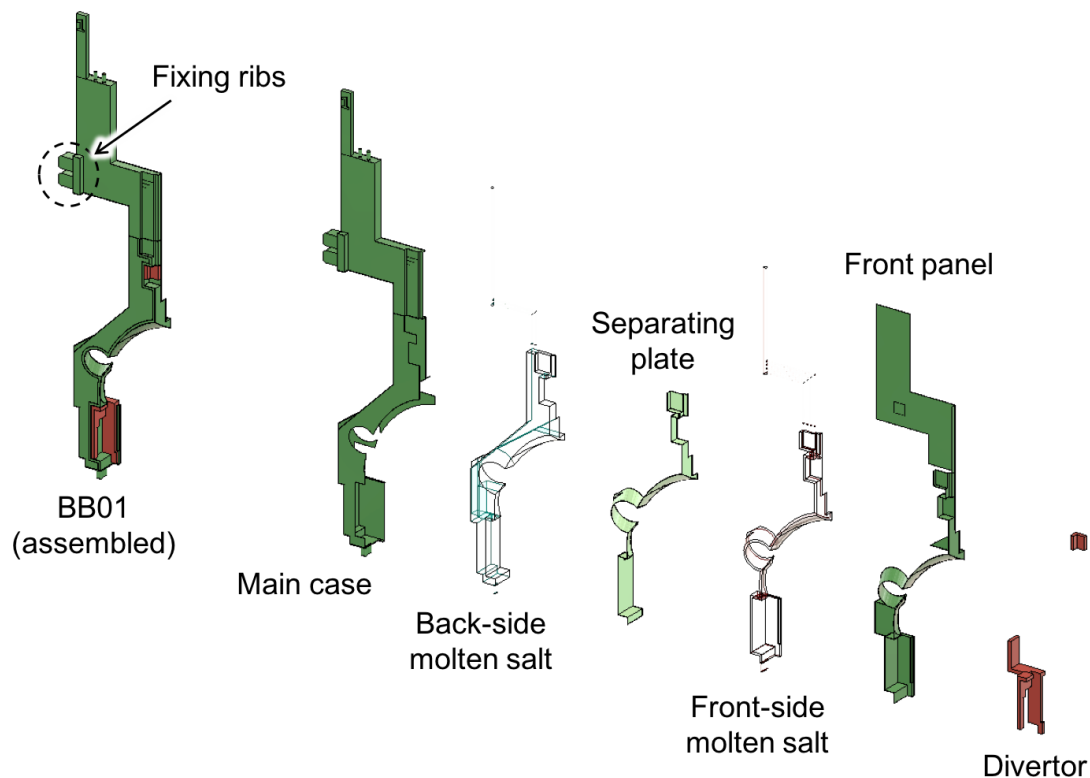


Fig. 6 An exploded view of BB01. The assembled form, the main case, the molten salt in the back-side, the separating plate, the molten salt in the front-side, the front panel, and the divertor are depicted from left to right.

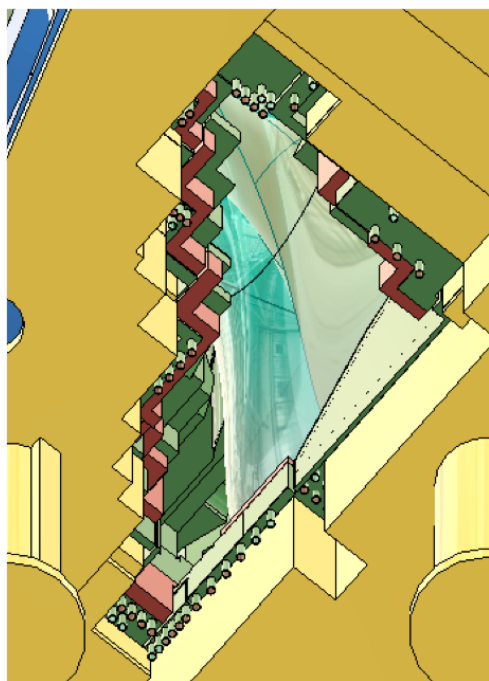


Fig. 7 Bottom view of the exhaust pipes equipped on the BB blankets.

and the thickness of walls and ribs will be performed in future by considering the complicated 3D structures of the BB cartridges.

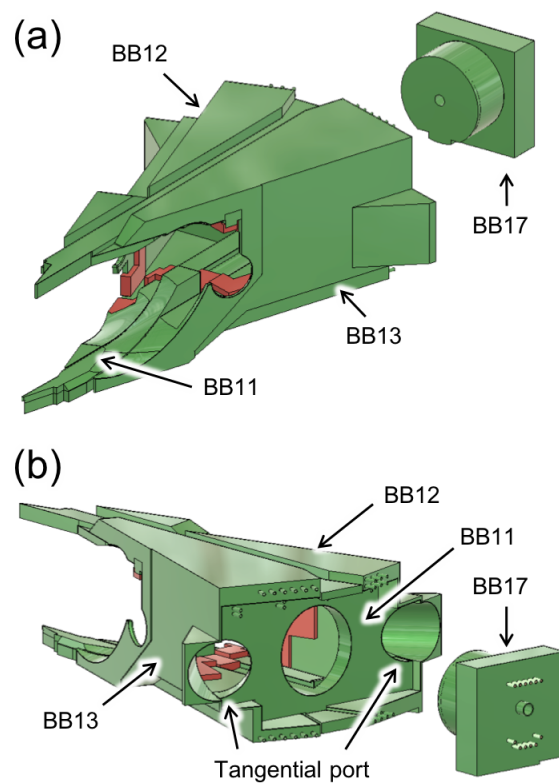


Fig. 8 (a) The front view and (b) the back view of the BB cartridges consisting of the outer port including two tangential ports.

Table 1 List of volumes and weights of the structure and molten salt in the BB cartridges.

Name	Volume of the structure (m ³)	Weight of the structure (ton)	Volume of the molten salt (m ³)	Weight of the molten salt (ton)	Total mass (ton)
BB01	0.08	0.65	0.24	0.47	1.12
BB02	0.12	0.93	0.27	0.54	1.47
BB03	0.12	0.93	0.44	0.88	1.81
BB04	0.08	0.67	0.08	0.16	0.83
BB05	0.10	0.81	0.29	0.58	1.39
BB06	0.11	0.91	0.21	0.41	1.33
BB07	0.14	1.13	0.36	0.72	1.85
BB08	0.19	1.53	0.27	0.54	2.07
BB09	0.26	2.05	1.18	2.36	4.41
BB10	0.13	1.03	0.69	1.37	2.40
BB11	0.08	0.61	0.54	1.08	1.69
BB12	0.11	0.88	0.48	0.96	1.83
BB13	0.14	1.11	0.61	1.22	2.33
BB14	0.14	1.14	0.00	0.00	1.14
BB15	0.04	0.31	0.00	0.00	0.31
BB16	0.11	0.90	0.00	0.00	0.90
BB17	0.03	0.24	0.17	0.34	0.57
Total	20	158	58	116	275

Volumes and weights of the structure and the molten salt in the BB cartridges are listed in Table 1. Here, the densities of structure material and molten salt are assumed to be 8 ton/m³ and 2 ton/m³, respectively. At maintenance, one should remove and reinstall the empty BB cartridges. Note that the molten salt is basically drained from the BB cartridges at maintenance. The heaviest cartridge is the BB09 of ~2 tons without molten salt. The total weight of 170 empty BB cartridges at all 10 sections is ~1,580 tons. When these are filled with the molten salt, the total weight of 170 BB cartridges increase to 2,750 tons.

4. The Neutron Shielding Blanket (SB)

Similar to the BB, the SB is also divided into several cartridges, as was already shown in Fig. 3. This makes it possible to shorten the construction period. All the SB cartridges except the SB01 are manufactured and tested in the factory. These are then transported to the construction site and assembled after the construction of the SC magnet coils is completed on the SB01. The CARDISTRY-B2 is composed of only 160 SB cartridges in total except the SB01. Therefore, even if it takes two days to install one SB cartridge, the total period for assembly can be shorter than one year.

Each SB cartridge is basically a box consisting of a main case and a back panel, as shown in Fig. 9 (and Figs. C1 - C8 in the Appendix). This box is filled with pebbles or small blocks of WC. The back panel is cooled to ~80 K by gas He. At the same time, the WC is also

cooled by gas He to maintain the BB side of the main case at around room-temperature. The filling rate of WC is assumed to be 40% to keep enough space for the coolant gas. Detailed estimations of the temperature profile of each SB cartridges, the resultant deformation and neutron streaming are remained for the future studies.

Volumes and weights of the structure and the WC in the SB cartridges are listed in Table 2. Here, the densities of structure material and WC are assumed to be 8 ton/m³ and 16 ton/m³, respectively. The weight of the WC is estimated by multiplying the volume, the density, and the filling rate of 40%. Note that the cartridges SB01, SB08, SB09, SB10, SB11, SB16, and SB17 (Fig. C1 in the Appendix) do not include the WC, since these are mainly used to form the outer structure of the SB that encloses the HTS magnet coils and forms a cryostat. Other SB cartridges surrounding the BB and the plasma contain the WC to enhance the neutron shielding rate. The total weight of the SB cartridges including the WC in all 10 sections is ~8,560 tons. Then, the sum of this and all BB cartridges is 11,310 tons.

5. Compatibility with the Divertor

The CARDISTRY-B2 is designed to be consistent with the liquid metal ergodic limiter/divertor named the REVOLVER-D (reactor-oriented effectively volumetric vertical divertor)[13], which is installed on each of the ten inner ports. Recently, we have changed the basic concept of the REVOLVER-D by replacing the molten tin shower with the solid tin pebbles, and renamed it as the

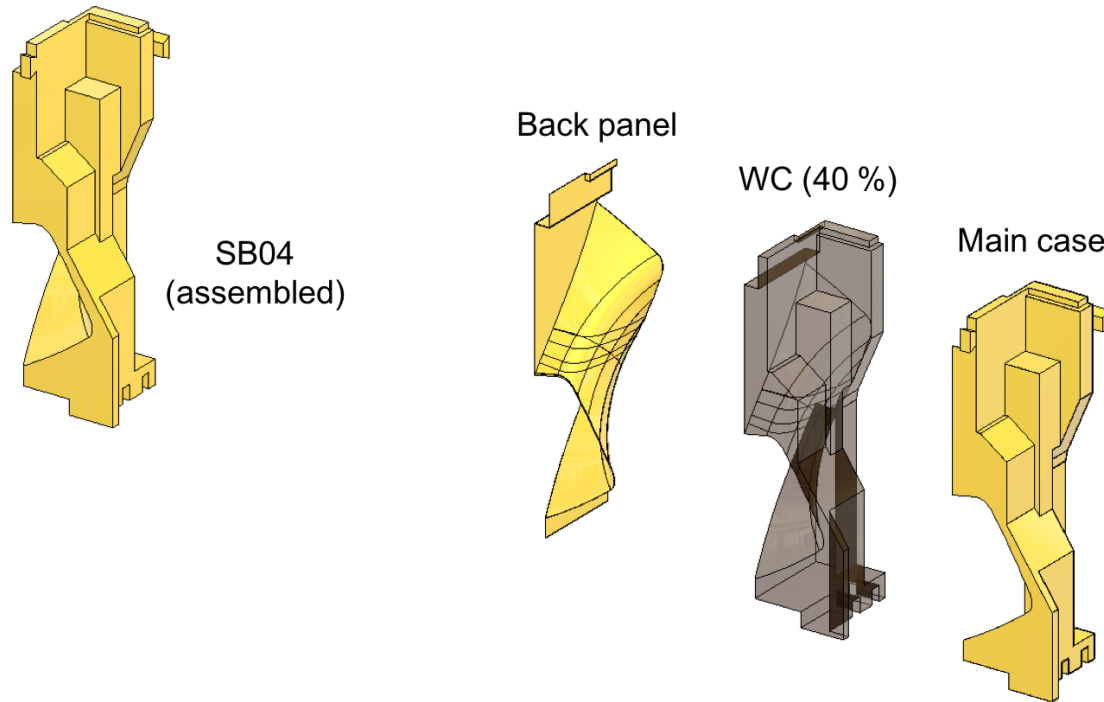


Fig. 9 An exploded view of SB04. The assembled form, the back panel, the tungsten-carbide of 40% filling rate, and the main case are depicted from left to right.

Table 2 List of volumes and weights of the structure and molten salt in the SB cartridges.

Name	Volume of the structure (m ³)	Weight of the structure (ton)	Volume of the WC (m ³)	Weight of the WC (ton)	Total mass (ton)
SB01	2.48	19.87	0.00	0.00	19.87
SB02	0.05	0.38	0.49	3.17	3.55
SB03	0.04	0.30	0.23	1.45	1.75
SB04	0.06	0.46	0.85	5.46	5.92
SB05	0.06	0.46	0.31	2.02	2.48
SB06	0.04	0.36	0.47	2.98	3.34
SB07	0.04	0.30	0.13	0.84	1.14
SB08	0.28	2.21	0.00	0.00	2.21
SB09	1.56	12.47	0.00	0.00	12.47
SB10	1.48	11.86	0.00	0.00	11.86
SB11	0.41	3.28	0.00	0.00	3.28
SB12	0.20	1.59	0.53	3.39	4.98
SB13	0.17	1.39	0.55	3.50	4.89
SB14	0.03	0.20	0.12	0.74	0.94
SB15	0.03	0.20	0.18	1.17	1.37
SB16	0.14	1.10	0.00	0.00	1.10
SB17	0.56	4.48	0.00	0.00	4.48
Total	76	609	39	247	856

REVOLVER-D2 [14]. The CARDISTRY-B2 is compatible with both the REVOLVER-D and the REVOLVER-D2. Furthermore, the helical divertor, which was not included in the former CARDISTRY-B, is now included in the design of the CARDISTRY-B2.

A schematic view of the tin pebble flow of the REVOLVER-D2 is depicted in Fig. 10. Tin pebbles transported to the top of the device by a vibratory spiral elevator fall through the BB14 and hit the plasma at the ergodic layer. The plasma becomes neutralized and evacuated

through the BB16. After that, tin pebbles further fall into the lower unit of the REVOLVER-D2, through the BB15. Some pebbles irradiated by the hot plasma may be damaged or melted. These damaged pebbles together with the pebbles without damage are melted in the pool of molten tin on the lower unit of the REVOLVER-D2. This molten tin pool absorbs the large impact of falling pebbles. The molten tin is introduced to the Si oil pool through a shower nozzle unit. Then, the molten tin droplets are cooled in the Si oil pool and become solid tin pebbles. The

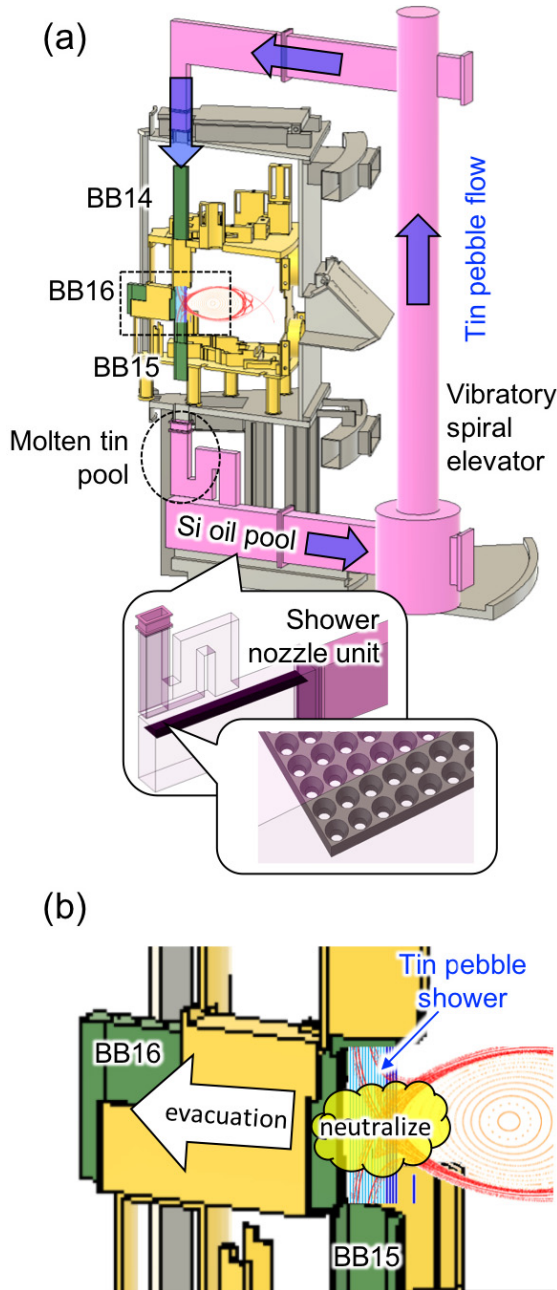


Fig. 10 (a) A bird's eye view of the REVOLVER-D2, where arrows denote the tin pebble flow, and (b) a close-up view of region enclosed by a broken square in (a).

solid tin pebbles are transported to the top of the device by the vibratory spiral elevator again and then repeat the same scenario.

Although the REVOLVER-D2 is expected to receive $\sim 90\%$ of the total divertor heat load [13], the remaining $\sim 10\%$ will hit the divertor foot prints determined by the magnetic field configuration. In the CARDISTRY-B2, water-cooled tungsten divertor units are equipped on each BB cartridge. A bird's eye view of the helical divertor units is shown in Fig. 11. Note that the detailed position of the divertor unit is not fixed yet. It should be determined ac-

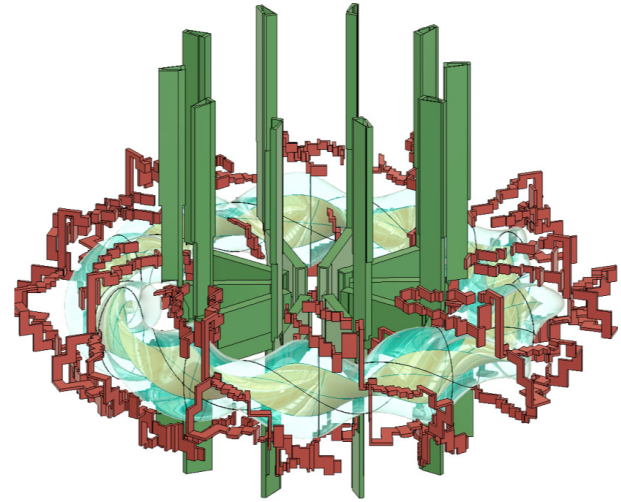


Fig. 11 A bird's eye view of the entire helical divertor equipped on the CARDISTRY-B2.

ording to the results of magnetic line trace calculation in the future. The divertor units are replaced together with the BB cartridges. Therefore, the lifetime of the divertor units determines the maintenance frequency of the BB. The divertor units are basically installed to the shaded regions with respect to the core plasma, where the direct 14 MeV DT neutron irradiation is small. This may help to realize a long-life divertor unit. A neutron transport simulation currently being prepared will clarify the lifetime of the divertor unit and therefore the maintenance schedule of the BB.

6. Summary

An improved design of the cartridge-type blanket system CARDISTRY-B2 has been proposed. This is based on the former design of the CARDISTRY-B. Similar to the former design, the CARDISTRY-B2 consists of BB and SB blanket cartridges that can be installed after the SC magnet coils are constructed. The CARDISTRY-B2 has solved several issues found in the former design as listed below:

- (1) the total number of the cartridges are largely reduced from 760 to 340,
- (2) tangential ports are equipped for the tangential NBI heating,
- (3) the helical divertor unit is set on each BB cartridge, and
- (4) extremely large bellows become unnecessary because the cryostat for the SC magnet coils is formed by the SB cartridges inside the vacuum vessel.

In the case of the CARDISTRY-B2 designed for the FFHR-b1, the total weight of the empty BB cartridges is 1,580 tons, which increases to 2,750 tons after the molten salt is filled. As for the SB cartridges, the total weight is 8,560 tons with WC of 40% filling rate. Then, the

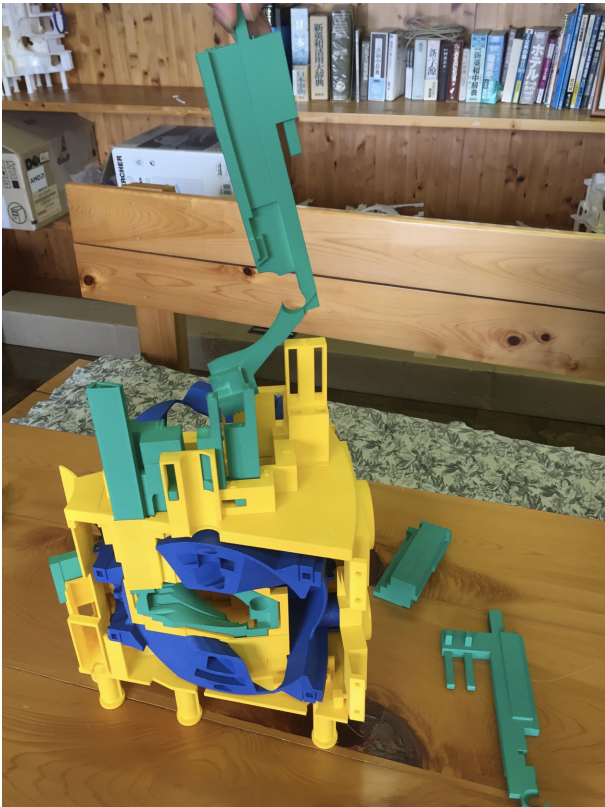


Fig. 12 A small model of the CARDISTRY-B2 for the FFHR-b1 of $\sim 1/20$ scale made by the 3D printing technology.

total weight of the CARDISTRY-B2 during operation is 11,310 tons.

It should be noted the detailed design of the CARDISTRY-B2 is not yet fixed. Further studies on the flow and thermal analyses together with the mechanical stress analysis are needed to determine the thickness of the structure material of the BB and SB blankets. The design of the separating plate in the BB cartridge should be reexamined after these analyses. The neutron transport should be carried out to evaluate the TBR and the neutron shielding rate. Although the CARDISTRY-B2 has a large coverage of $\sim 97\%$, the thickness of the BB is not necessarily large enough, which is 10 cm at the smallest. It is quite important to clarify whether $TBR > 1$ is possible or not in the CARDISTRY-B2 for the FFHR-b1. A numerical simulation on magnetic field line tracing is needed to determine the divertor position. Motion analyses of the BB car-

tridges at removal and reinstallation are also needed to determine the maintenance scenario. As in the former study on the CARDISTRY-B [6], a small 3D model of 28/625 ($= 0.0448$) $\sim 1/20$ scale is made by using the 3D printing technology, as shown in Fig. 12. Although 3D motion is needed to install/remove the SB and BB cartridges, it has been already confirmed to be possible using this 3D model. However, compared with the former CARDISTRY-B, where the SB and BB cartridges can be installed or removed with the 2D motion alone, it becomes difficult to describe the mechanical motion of robots or cranes for maintenance in the case of the CARDISTRY-B2. How to fix the BB blankets to the fixing units also remains for future study.

Acknowledgments

This work was supported by JSPS KAKENHI Grant Number 16K14530, and the budgets of NIFS15UFFF038 and NIFS17UFFF040 of the National Institute for Fusion Science.

Appendix

Figures that are not included in the main body of this article are summarized in this appendix, where side views of the assembled SB and BB with Poincaré plots of the ergodic layer and closed magnetic surfaces inside the LCFS (Figs. A1 - A4), exploded views of BB cartridges (Figs. B1 - B12) and SB cartridges (Figs. C1 - C8) are shown.

- [1] A. Sagara *et al.*, Nucl. Fusion **57**, 086046 (2017).
- [2] A. Komori *et al.*, Fusion Sci. Technol. **58**, 1 (2010).
- [3] J. Miyazawa *et al.*, Fusion Eng. Des. **136**, 1278 (2018).
- [4] J. Miyazawa *et al.*, Fusion Eng. Des. **146**, 2233 (2019).
- [5] Y. Someya *et al.*, Fusion Eng. Des. **124**, 615 (2017).
- [6] J. Miyazawa *et al.*, Plasma Fusion Res. **12**, 1405017 (2017).
- [7] T. Goto *et al.*, Plasma Fusion Res. **11**, 2405047 (2016).
- [8] T. Murase *et al.*, Fusion Eng. Des. **136**, 106 (2018).
- [9] S. Hong *et al.*, 13th ISFNT (25-29 Sep., 2017, Kyoto, Japan), P3-107.
- [10] A. Loving *et al.*, Fusion Eng. Des. **89**, 2246 (2014).
- [11] H. Utoh *et al.*, Fusion Eng. Des. **124**, 596 (2017).
- [12] D.A. Petti *et al.*, Summary Report of Japan-US Joint Project (JUPITER-II) (FuY 2001-2006) NIFS-PROC-71, 74 (2008). <http://www.nifs.ac.jp/report/nifs-proc71.html>
- [13] J. Miyazawa *et al.*, Fusion Eng. Des. **125**, 227 (2017).
- [14] T. Ohgo *et al.*, Plasma Fusion Res. **14**, 3405050 (2019).

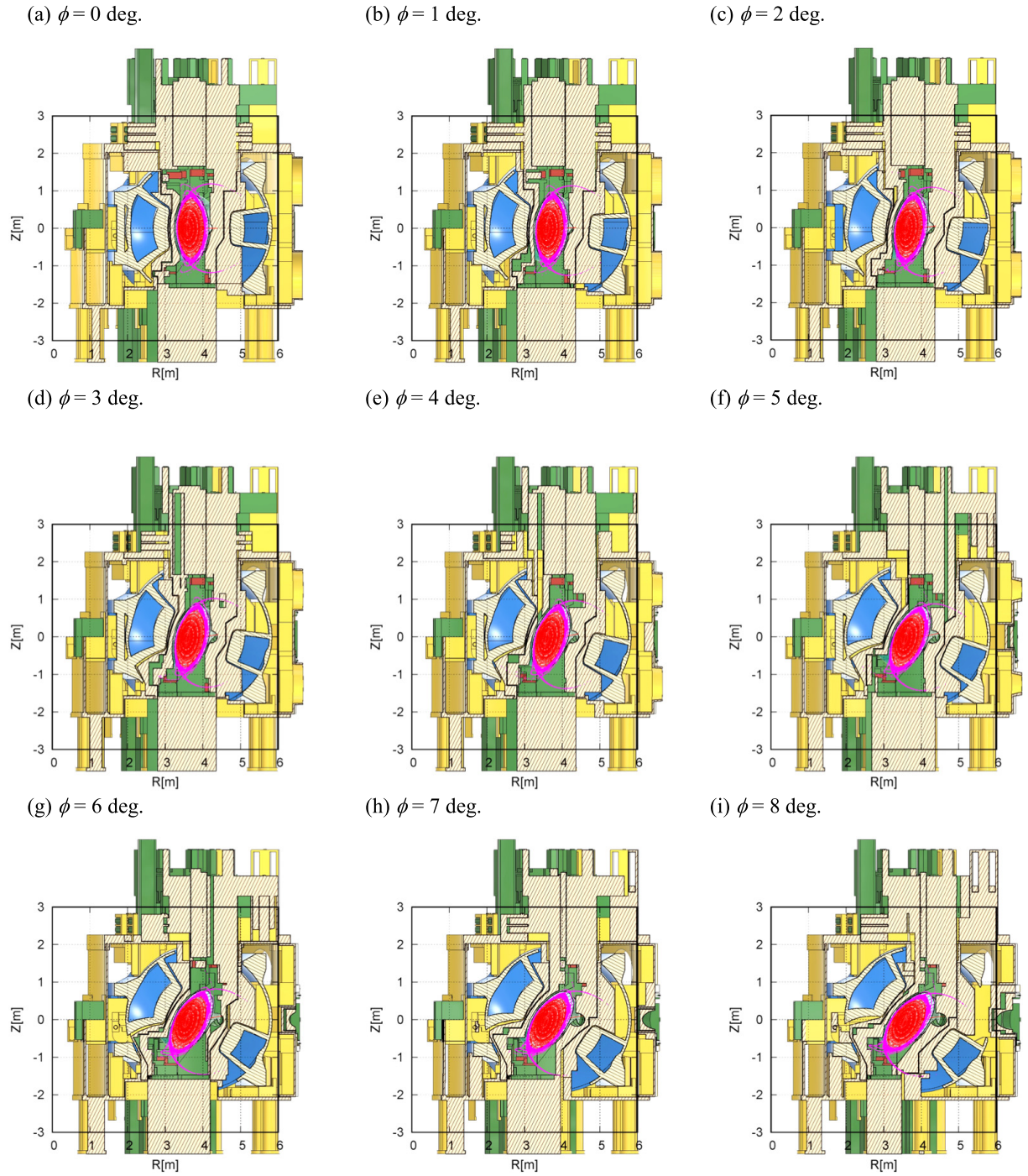


Fig. A1 Side views of the Poincaré plots of the magnetic field lines with the SB and the BB cartridges of the CARDISTRY-B2 sliced at the toroidal angle $\phi = 0 - 8$ deg.

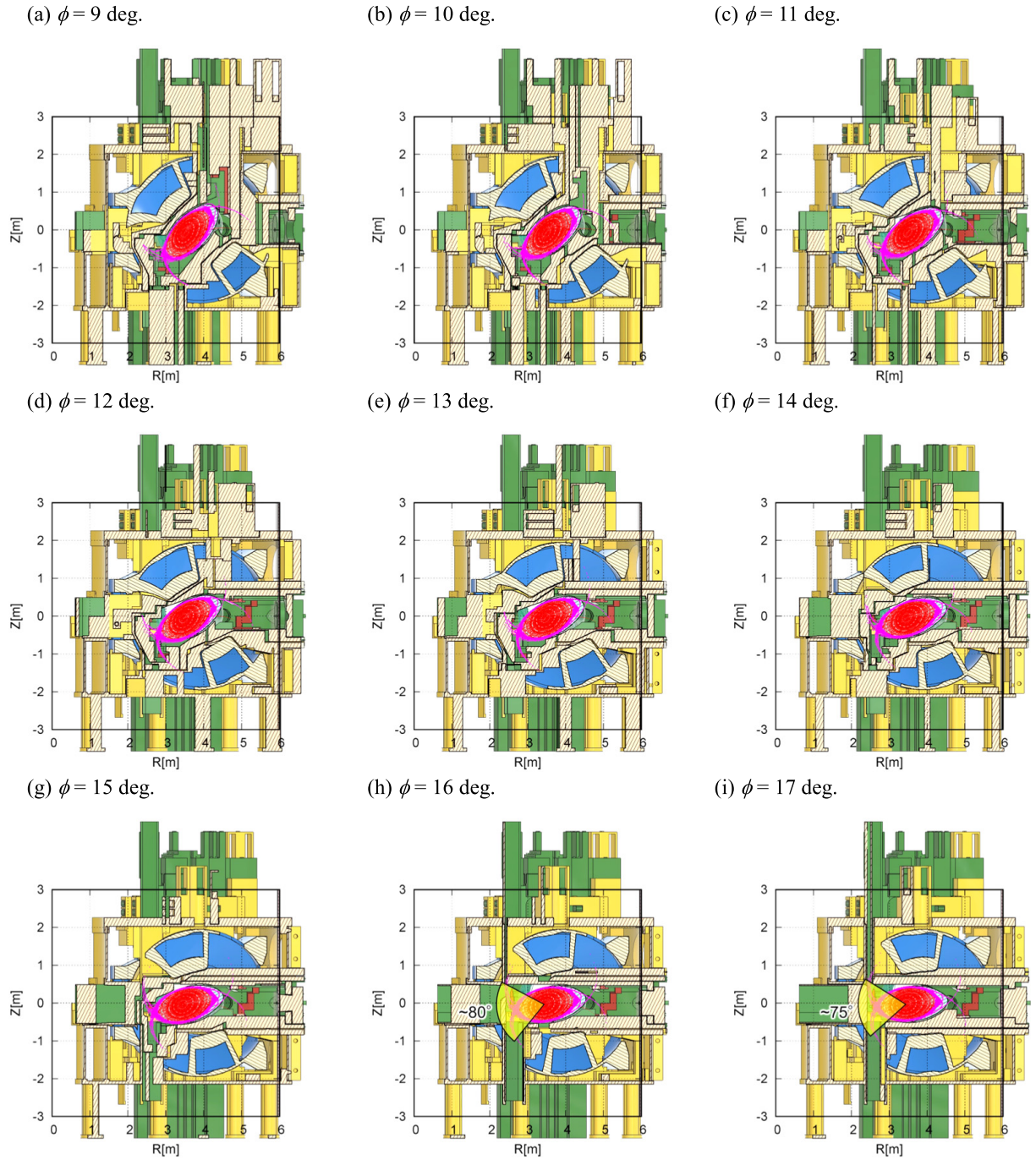


Fig. A2 Side views of the Poincaré plots of the magnetic field lines with the SB and the BB cartridges of the CARDISTRY-B2 sliced at the toroidal angle $\phi = 9 - 17$ deg.

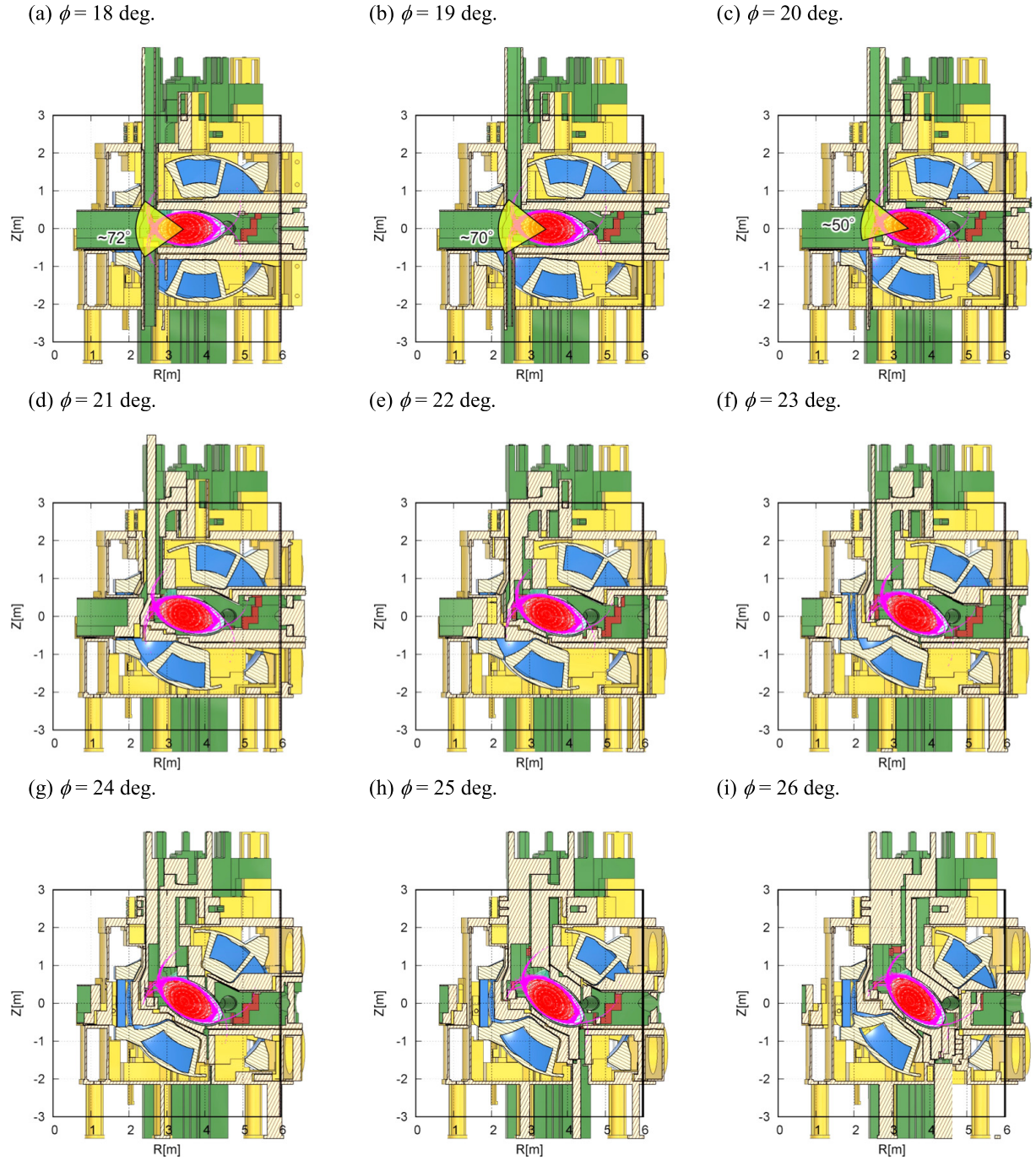


Fig. A3 Side views of the Poincaré plots of the magnetic field lines with the SB and the BB cartridges of the CARDISTRY-B2 sliced at the toroidal angle $\phi = 18 - 26$ deg.

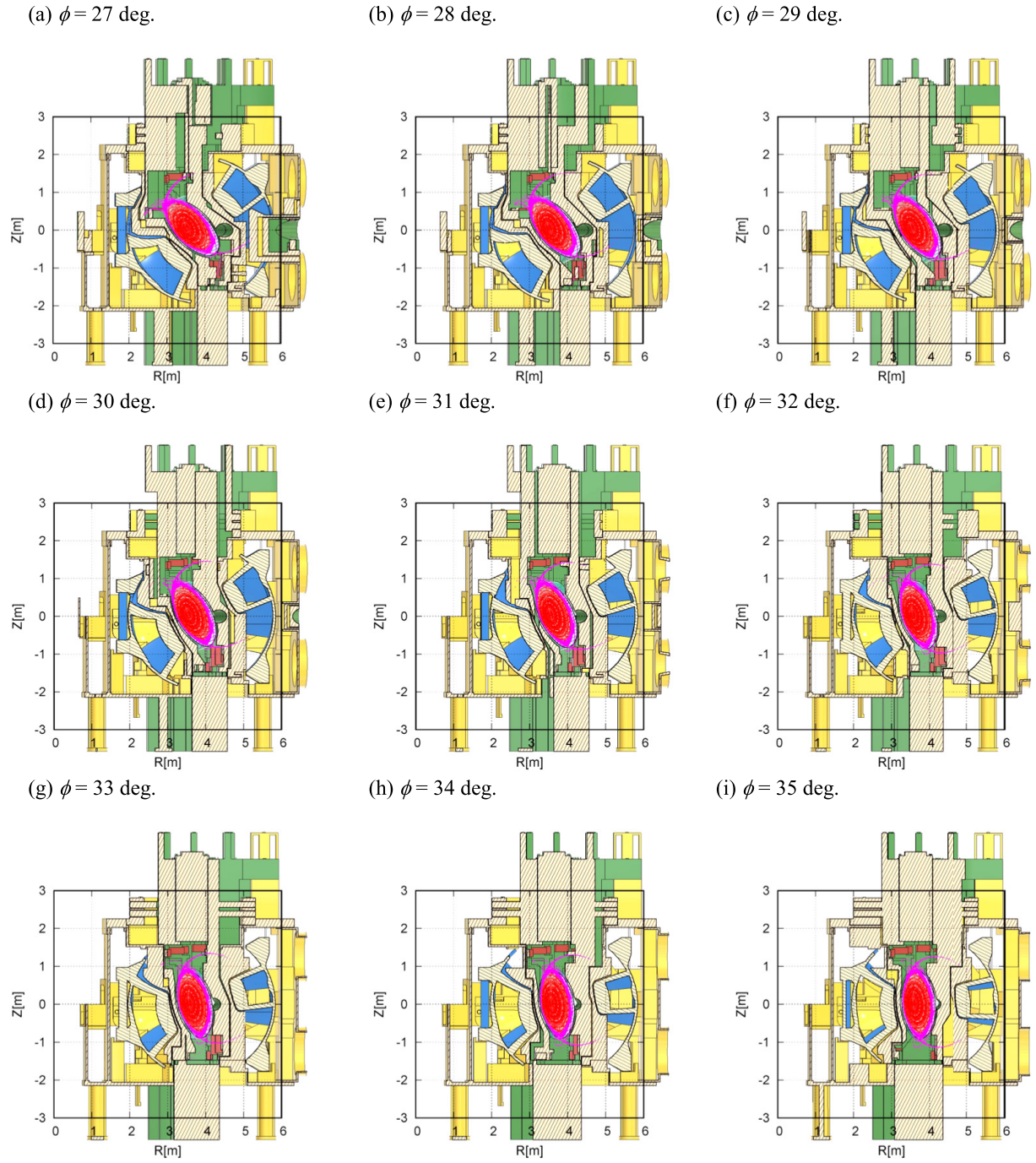


Fig. A4 Side views of the Poincaré plots of the magnetic field lines with the SB and the BB cartridges of the CARDISTRY-B2 sliced at the toroidal angle $\phi = 27 - 35$ deg.

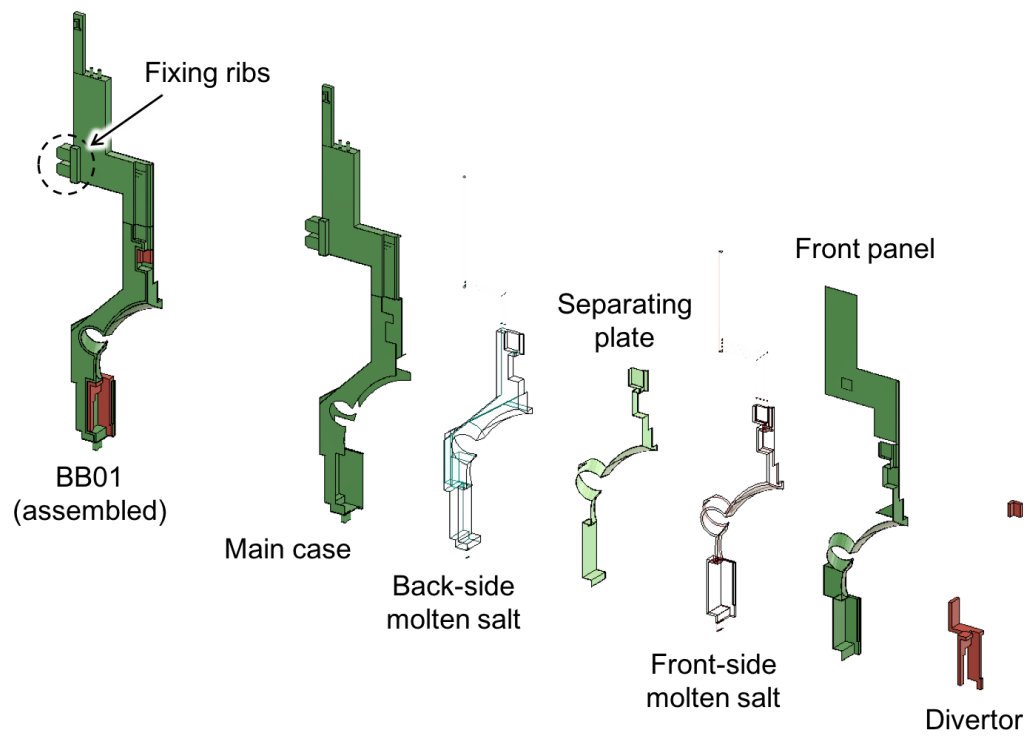


Fig. B1 An exploded view of BB01 (same as Fig. 6).

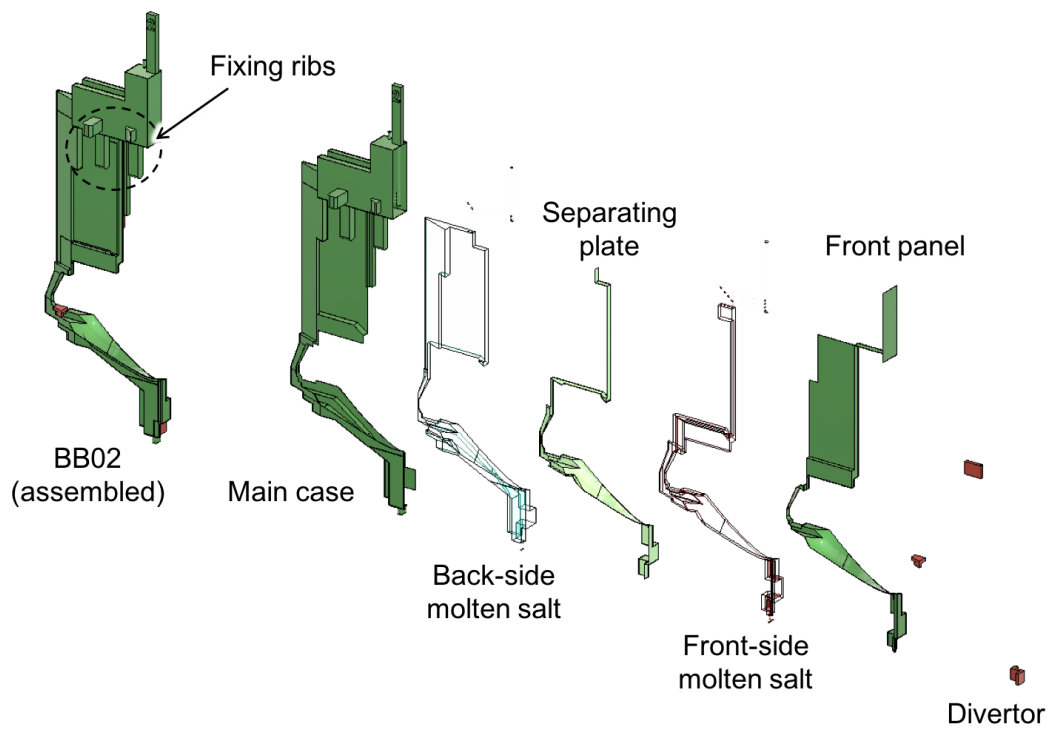


Fig. B2 An exploded view of BB02.

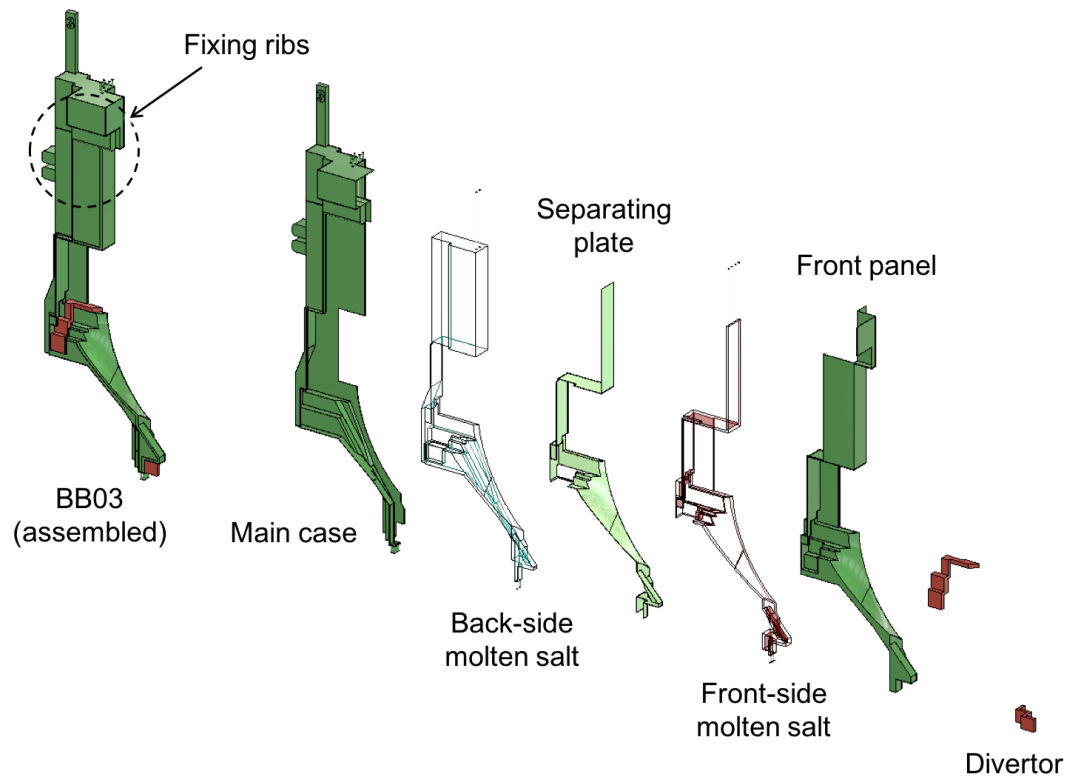


Fig. B3 An exploded view of BB03.

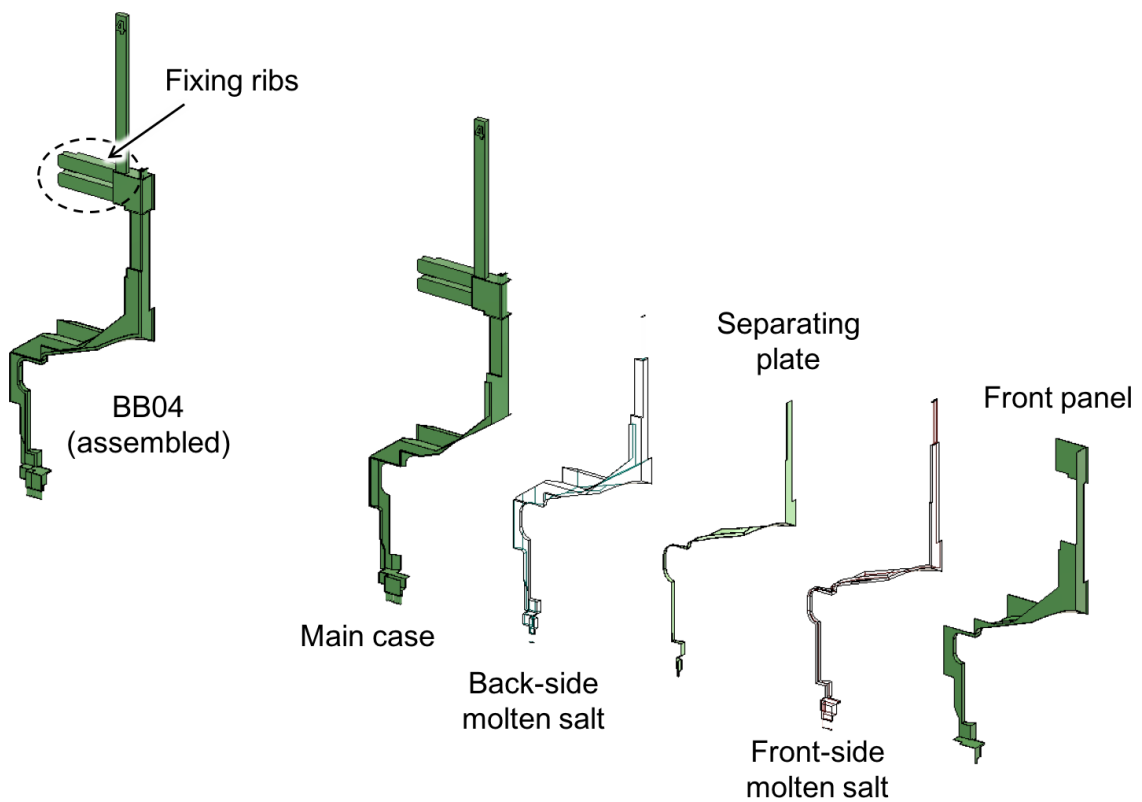


Fig. B4 An exploded view of BB04.

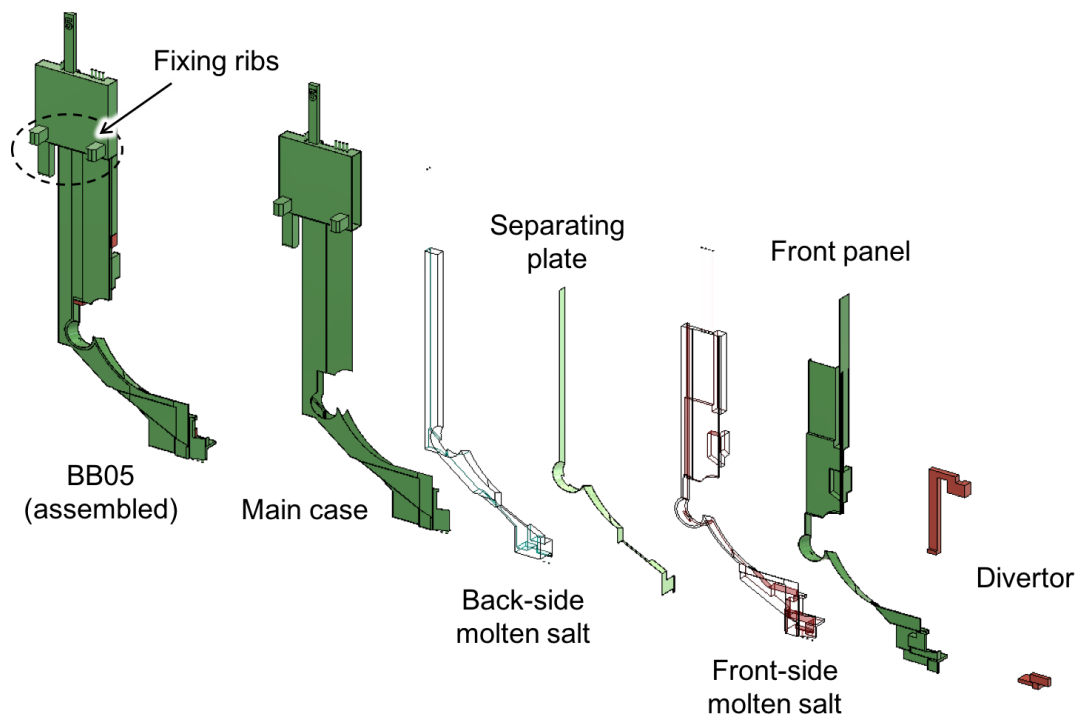


Fig. B5 An exploded view of BB05.

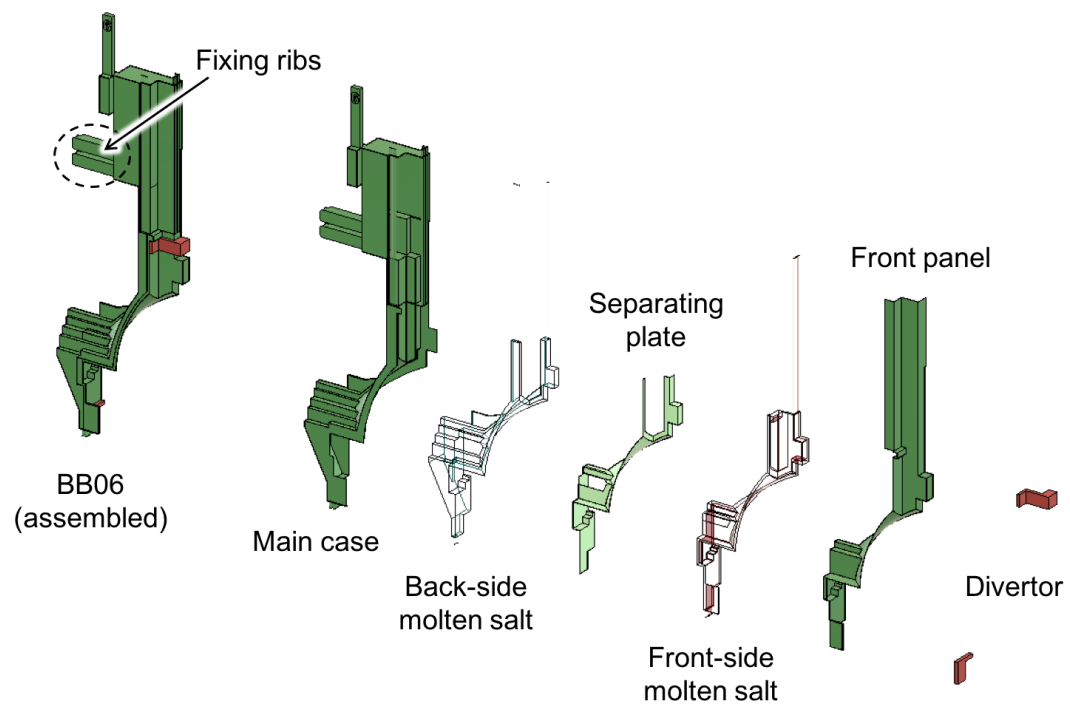


Fig. B6 An exploded view of BB06.

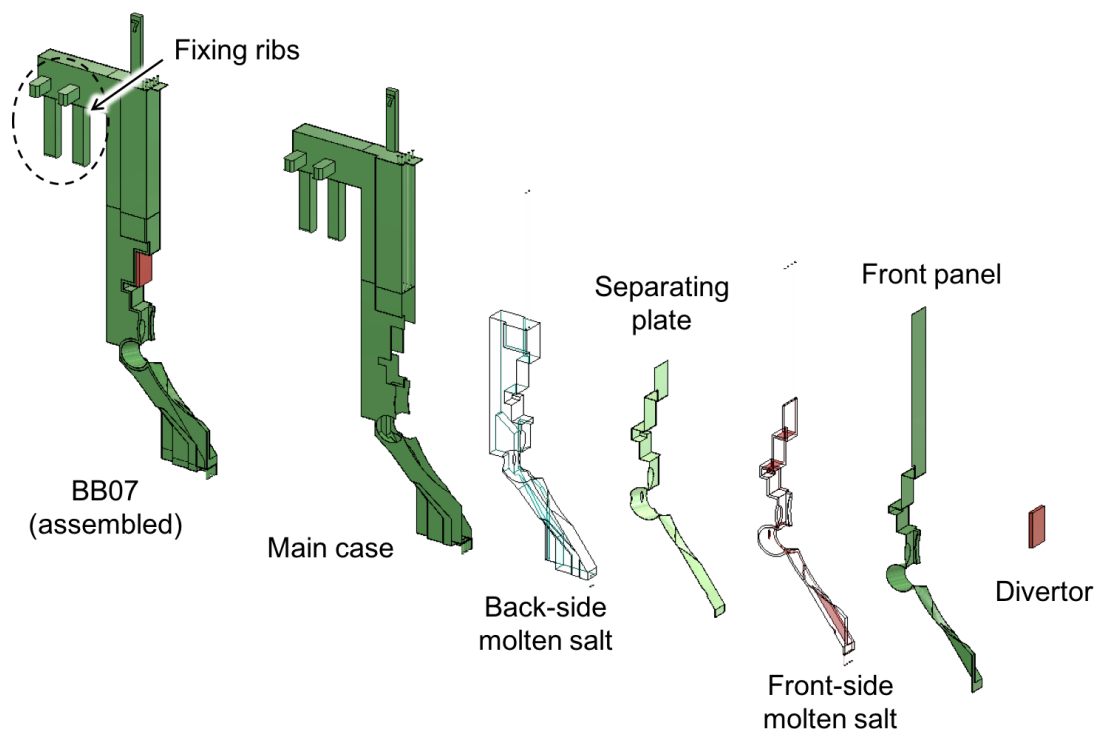


Fig. B7 An exploded view of BB07.

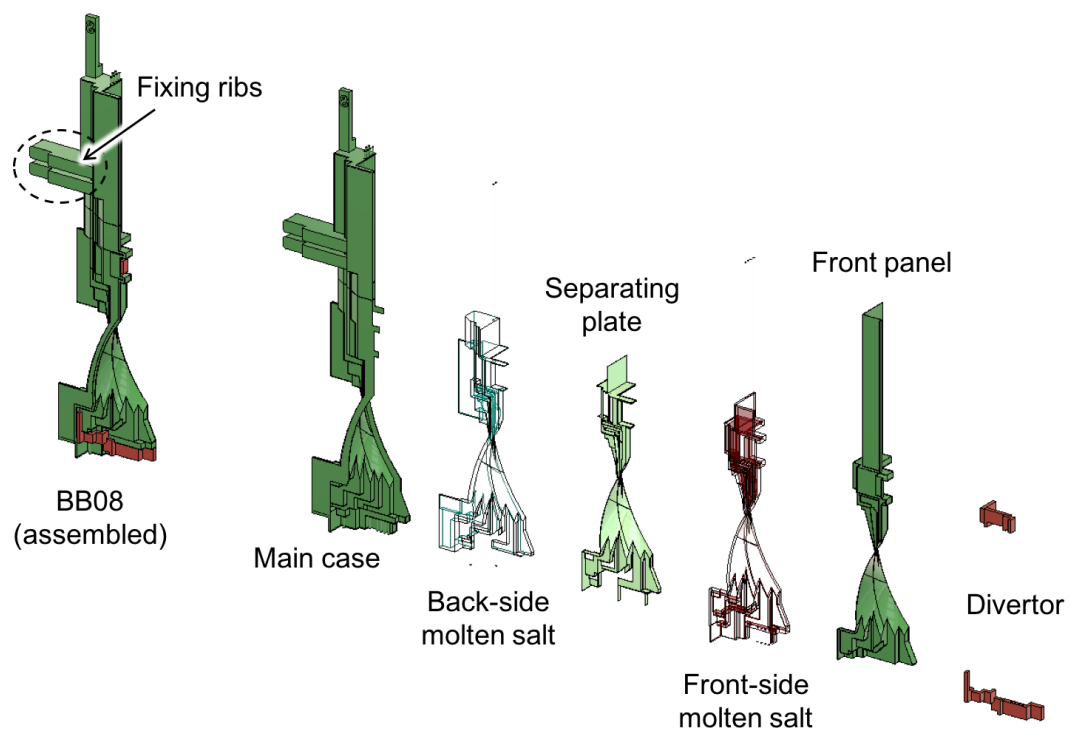


Fig. B8 An exploded view of BB08.

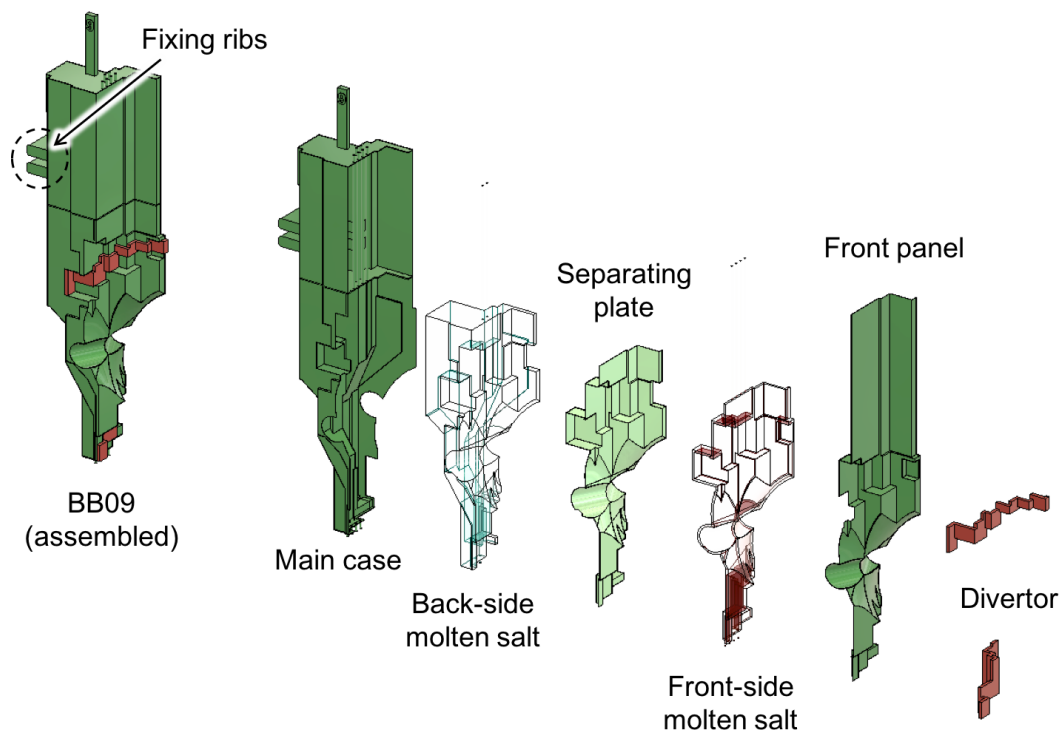


Fig. B9 An exploded view of BB09.

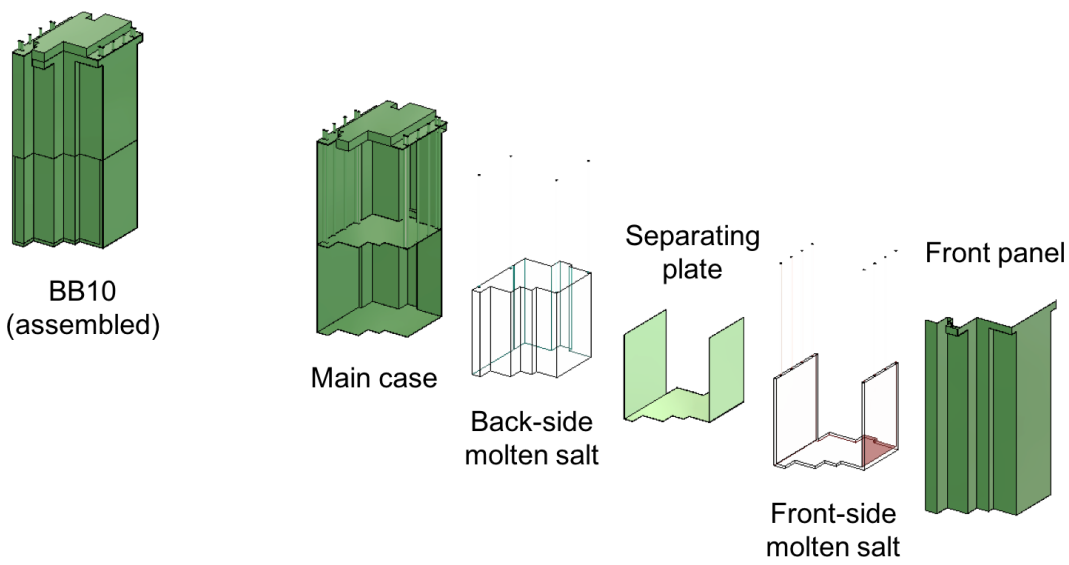


Fig. B10 An exploded view of BB10.

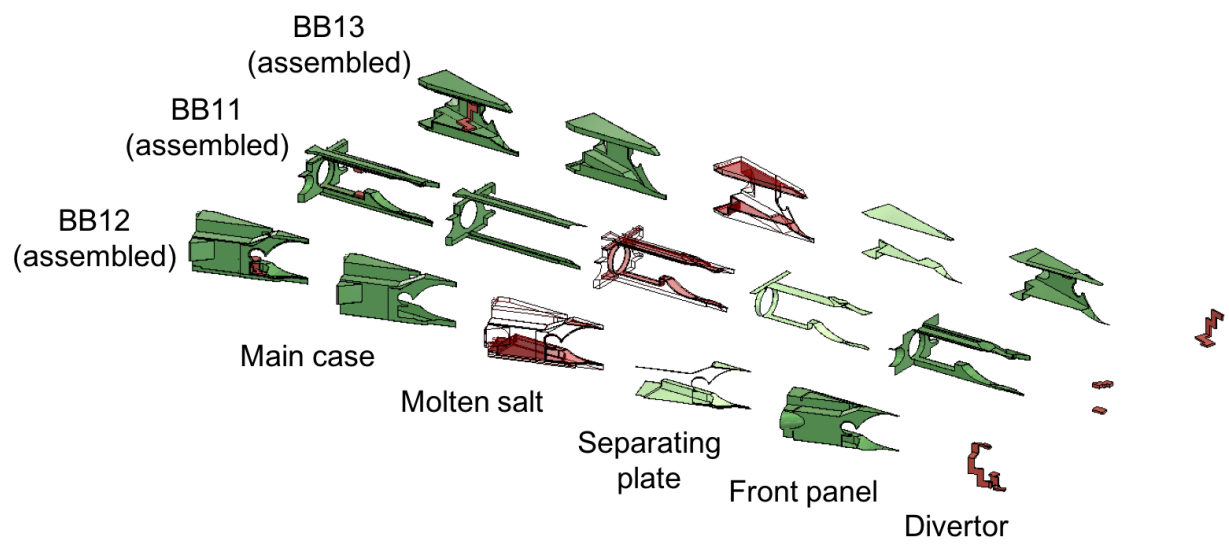


Fig. B11 Exploded views of BB11, BB12, and BB13.

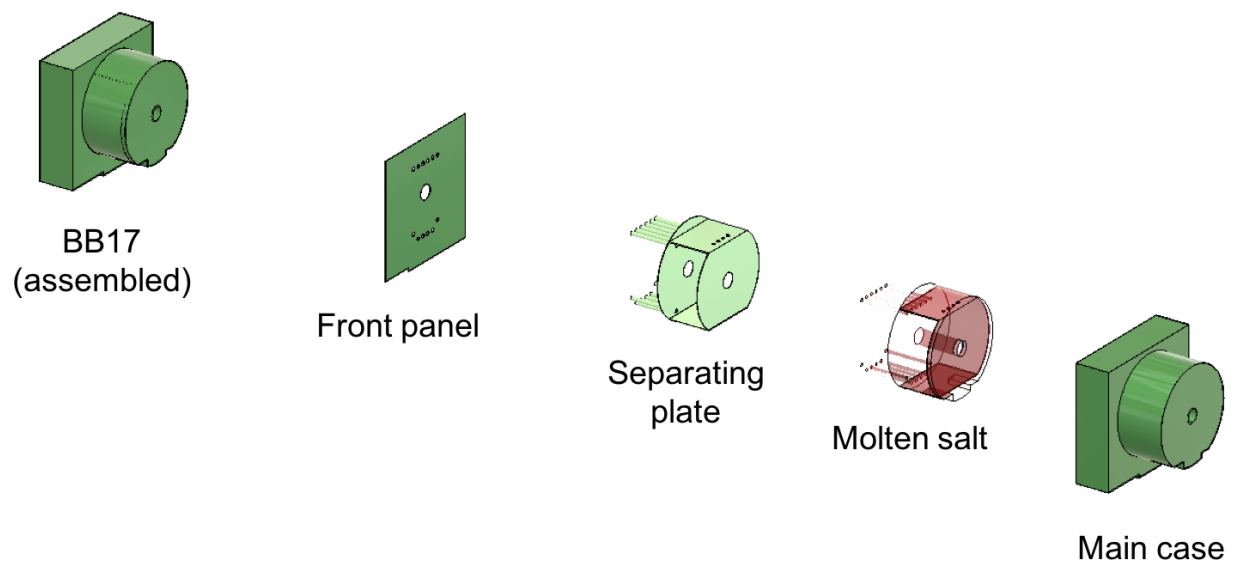


Fig. B12 An exploded view of BB17.

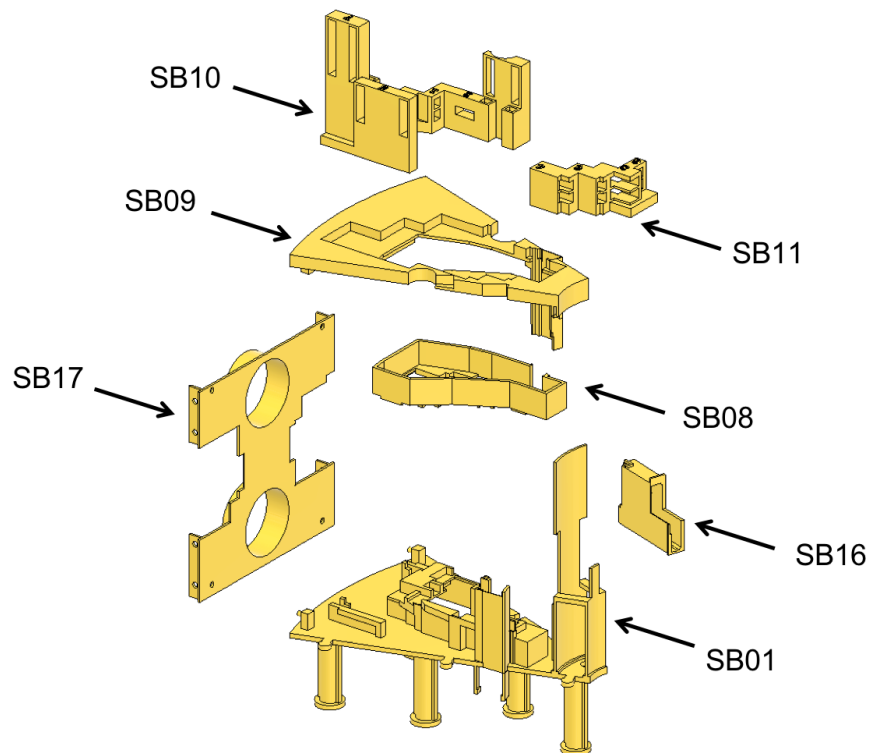


Fig. C1 An exploded view of SB01, SB08, SB09, SB10, SB11, SB16, and SB17.

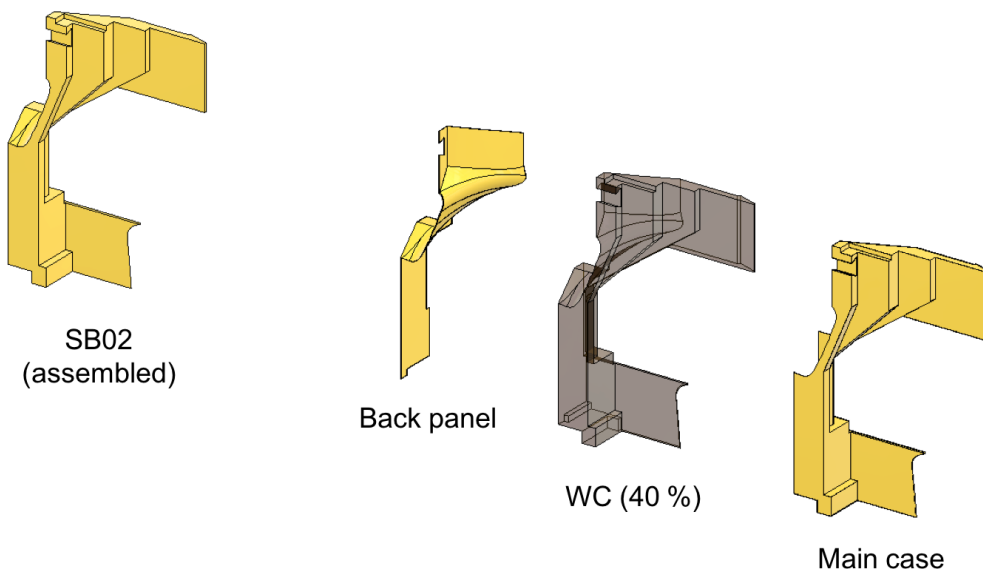


Fig. C2 An exploded view of SB02.

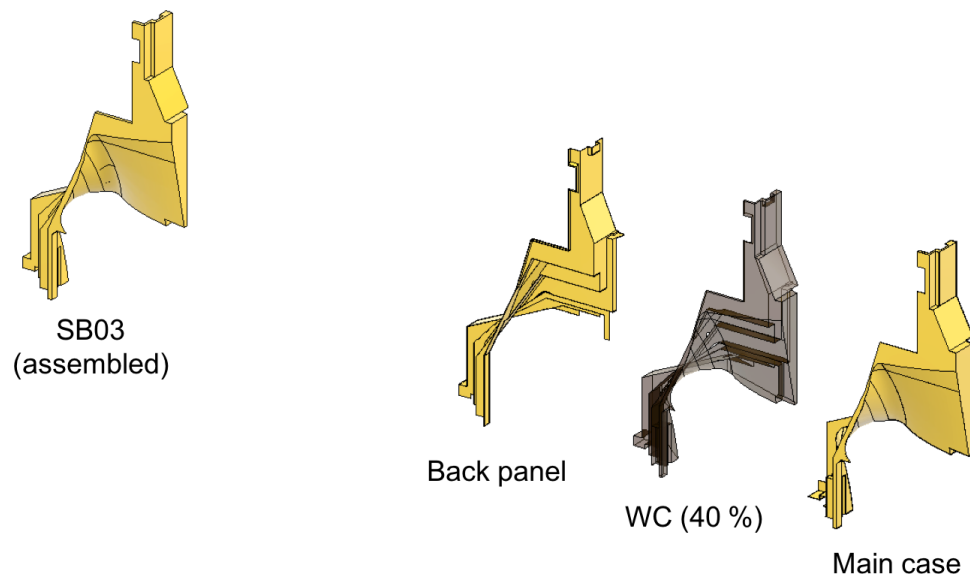


Fig. C3 An exploded view of SB03.

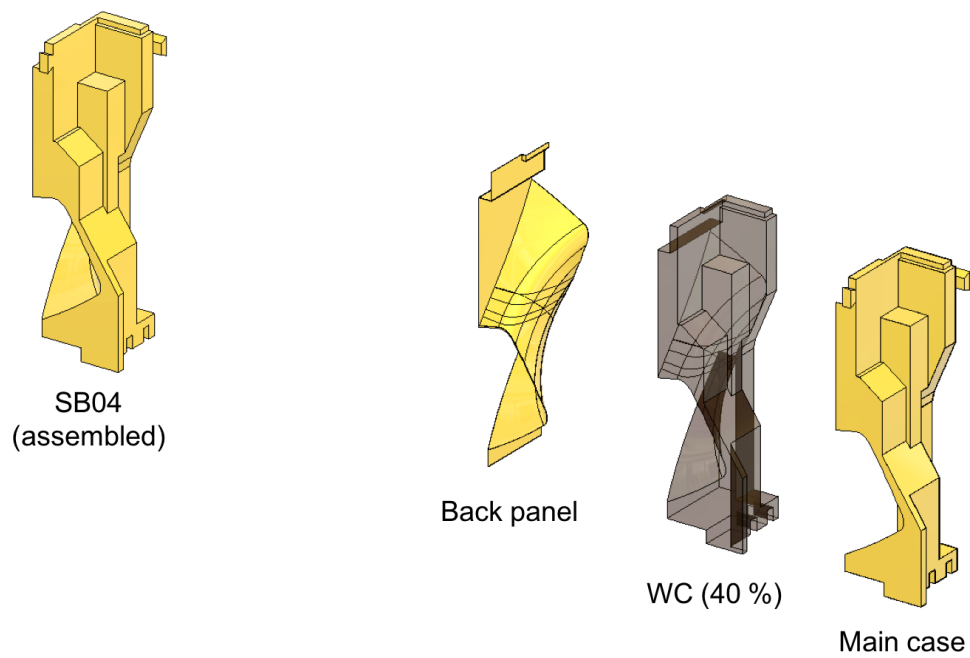


Fig. C4 An exploded view of SB04 (same as Fig. 9).

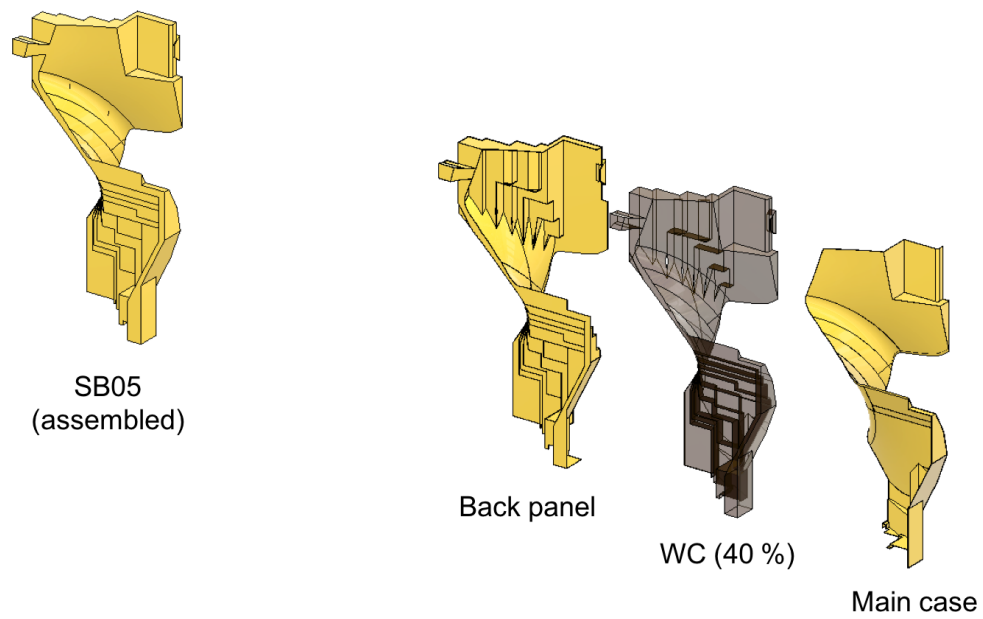


Fig. C5 An exploded view of SB05.

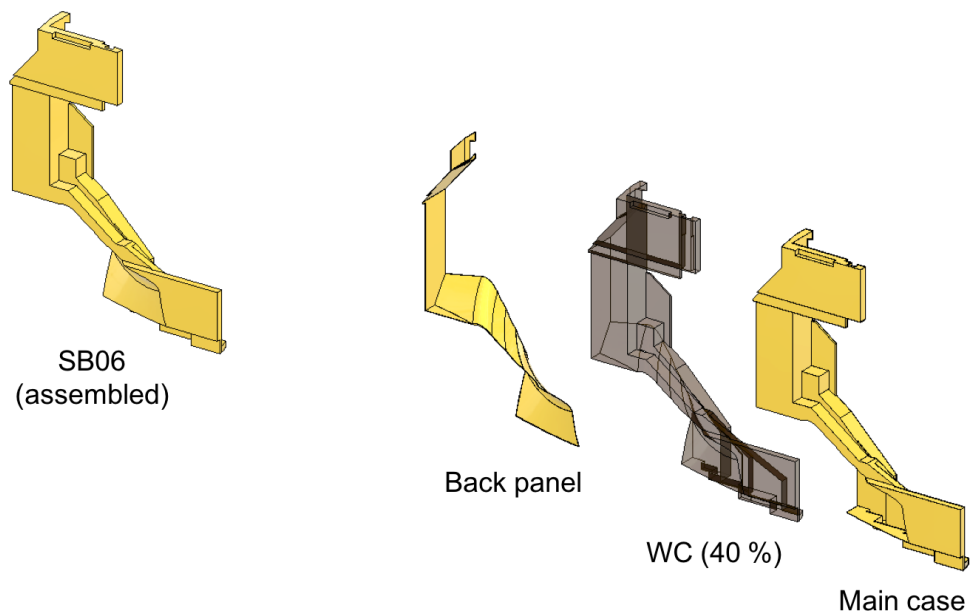


Fig. C6 An exploded view of SB06.

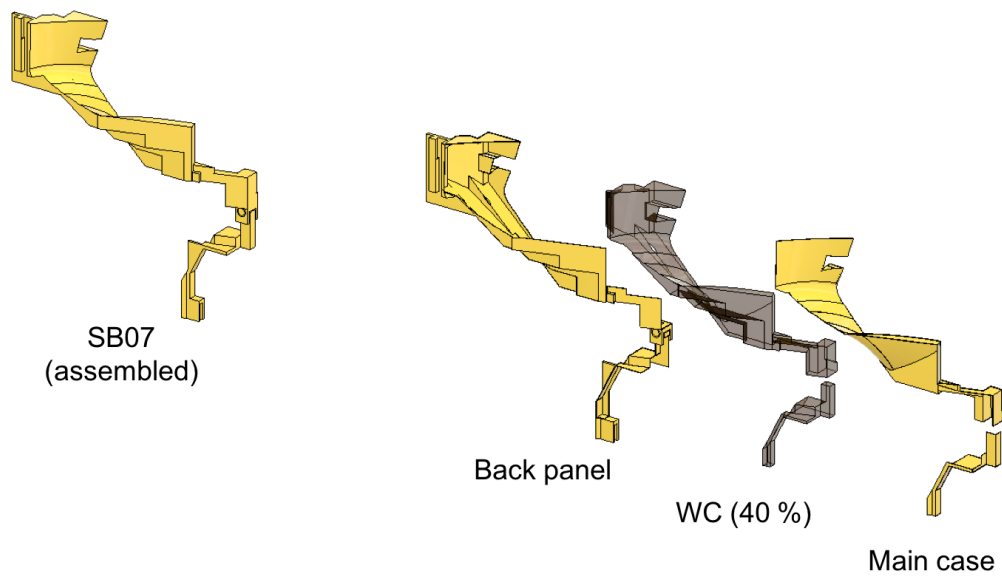


Fig. C7 An exploded view of SB07.

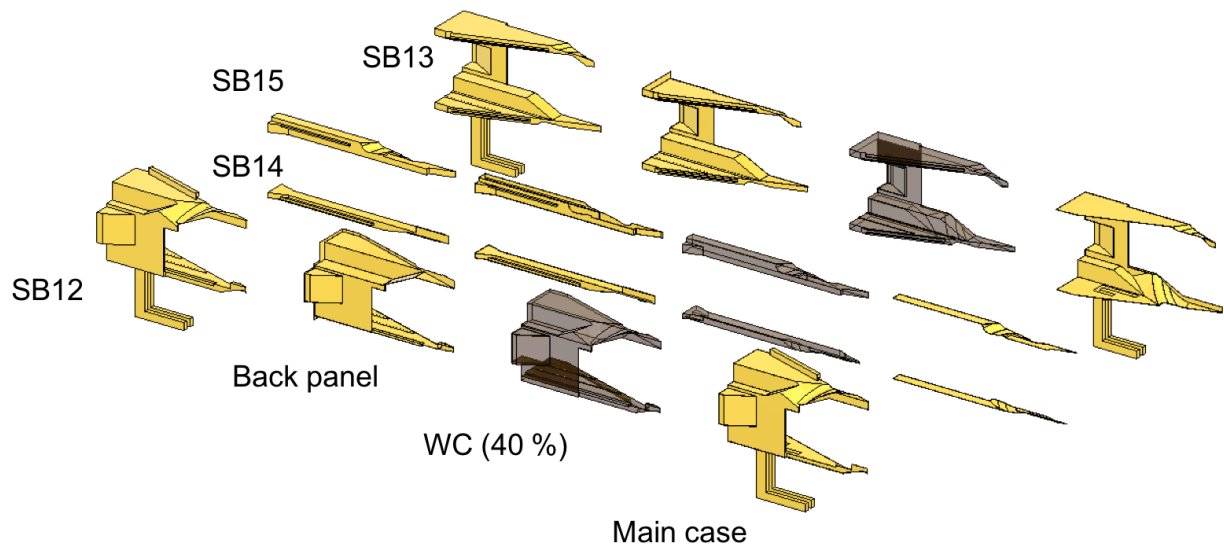


Fig. C8 Exploded views of SB12, SB13, SB14, and SB15.